The Nrf2-NLRP3-Caspase1 axis mediates the neuroprotective effects of Celastrol in Parkinson's disease

Chenyu Zhang
Peking University Health Science Centre
Miao Zhao
Peking University Health Science Centre
Bingwei Wang
Peking University Health Science Centre
Zhijie Su
Peking University Health Science Centre
Bingbing Guo
Peking University Health Science Centre
Ruimao Zheng (rmzheng@pku.edu.cn)
Peking University

Research article

Keywords: Parkinson's disease, Celastrol, Nrf2, NLRP3, Caspase1, α-synuclein

Posted Date: August 7th, 2020

DOI: https://doi.org/10.21203/rs.3.rs-50111/v1

Abstract

Background: Parkinson's disease (PD) is characterized by the loss of dopaminergic neurons in the substantia nigra pars compacta (SNc), accompanied by chronic neuroinflammation, oxidative stress, and widespread accumulation of α-synuclein. Celastrol (Cel), a potent anti-inflammatory and anti-oxidative pentacyclic triterpene, has emerged as a neuroprotective agent. However, the mechanisms by which celastrol is neuroprotective in PD has not yet been elucidated.

Methods: The MPTP and AAV-mediated human wild-type α-syn overexpression within SNc induced PD mouse models were employed in this study. By using multiple genetically modified mice (Nrf2-KO, NLRP3-KO and Caspase1-KO), we identified that celastrol effectively inhibited the NLRP3 inflammasome activation, mitigated motor deficits and nigrostriatal dopaminergic degeneration through Nrf2-NLRP3-Caspase1 pathway.

Results: Here we show that celastrol protected against the loss of dopaminergic neurons, mitigated the neuroinflammation and motor deficits in both MPTP-induced PD mouse model and AAV-mediated human α-syn overexpression PD model. Whole-genome deep sequencing analysis reveals that Nrf2, NLRP3 and Caspase1 in SNc may be associated with the neuroprotective actions of celastrol in PD.

Conclusions: These findings suggest that Nrf2-NLRP3-Caspase1 axis may be a key target of celastrol in PD treatment, and highlight the favorable properties linked to neuroprotection of celastrol, making celastrol as a promising disease-modifying agent for PD.

Background

Parkinson's disease (PD) is the second most common neurodegenerative disease, affecting about 2% of the population older than the age of 60, and the incidence of PD is expected to increase along with the population ages [1, 2]. The pathological hallmark of PD is the progressively loss of dopaminergic neurons in substantia nigra pars compacta (SNc), accompanying with the accumulation of misfolded α-synuclein in Lewy bodies, which decreases striatal dopamine, and thus leads to motor dysfunction, including resting tremors, bradykinesia and rigidity [2-4]. Although the pathology of PD remains unclear, compelling evidence from clinical, preclinical, and epidemiological studies suggests that neuroinflammation and oxidative stress may play central roles in PD pathogenisis [3, 5, 6]. To date, despite substantial efforts, there is still no disease-modifying agent to prevent the progression of PD; and gene therapy clinical trials for PD also failed to halt or slow the disease process of PD [7, 8, 9]. Therefore, there's an urgent need to discover new therapeutic agents to protect against the loss of dopaminergic neurons in PD. In light of this, the development of promising agents exhibiting disease-modifying properties is critical.

Notably, natural products show a promising role in the development of novel agents for PD treatment due to both their pharmacological properties linked to neuroprotection and medication safety [10], including squalamine, ursolic acid and boswellic acid [10, 11]. Celastrol, a pentacyclic triterpene, is an active component of *tripterygium wilfordi* (thunder god vine). Celastrol has shown favorable neuroprotective

properties in neurodegenerative disease (Alzheimer's disease, Parkinson's disease, and Huntington's diseases) because of its anti-oxidative and anti-inflammatory effects [12-14]. A series of studies suggest that celastrol can protect against the neurotoxins-induced loss of dopaminergic neurons (MPTP and rotenone) [12, 15], suppress the activation of microglia, reduce the production of neuroinflammatory cytokines, and inhibit the induced nitric oxide generation by iNOS [13, 16]. Besides, celastrol can promote autophagy [12], ameliorate the mitochondrial dysfunction [17], and inhibit lipid peroxidation induced by ADP and Fe^{2+} [18]. Together, these evidence suggests that the multiple pharmacological effects of celastrol correspondence the pathogenesis of PD, which raise the possibility that celastrol might be a promising candidate for the treatment of PD. However, the mechanism underlying the neuroprotective action of celastrol remains unclear.

To investigate the potential mechanisms underlying the neuroprotective role of celastrol in PD, we initially performed whole-genome deep sequencing analysis to explore the differential expression genes (DEGs) in the SNc of celastrol-treated PD mouse model. Notably, this unbiased high-throughput approach enables the identification of genes associated with the neuroprotective effects of celastrol, such as *Nrf2, HO1, Nlrp3, Caspase1 and ASC*. Nrf2 (nuclear-factor-E2-related factor 2), a nuclear Cap-n-Collar basic region leucine zipper transcription factor, is a key transcription factor which plays a critical role in PD pathogenesis [19]. Under normal conditions, Nrf2 resides in cytosol and is dissociated by ubiquitination and proteolytic degradation; under the condition of PD-causing toxins (rotenone and MPTP), Nrf2 can translocate to the nucleus where it binds to antioxidant response element (ARE) to induce antioxidant and phase II detoxification enzymes, and then exhibits profoundly anti-oxidative and anti-inflammatory effects [20, 21]. Human genetic studies show that a functional haplotype in the Nrf2 gene promoter (GAGCAAAA), confers high transcriptional activity and decreased incidence of PD in Swedish and Polish PD patients [22, 23]. Notably, selegiline (deprenyl), a type-B monoamine oxidase (MAO-B) inhibitor, which is currently used in the treatment of PD, also displays anti-oxidative effect via the activation of Nrf2 [24]. Moreover, it's reported that overexpression of Nrf2 protects against motor pathology and α-synuclein aggregation [25]; whereas deficiency of Nrf2 exacerbates PD phenotypes in mice [20, 22]. Recent studies have revealed that celastrol relieves inflammation in diet-induced obese mice via the regulation of Nrf2 [26]. Newly discovered evidence suggests that natural products, including berberine and icariin, exert anti-oxidative and anti-inflammatory effects via the activation of Nrf2 [27, 28]. However, whether the neuroprotective action of celastrol is dependent on the activation of Nrf2 remains unknown.

NLRP3 (NACHT, LRR and PYD domains-containing protein 3), a cytosolic protein, belongs to critical inflammatory signaling complex called inflammasome, which participates in the pathogenesis of PD [2, 29]. Extensive microglial activation and NLRP3 inflammasome activation have been observed in the SNc of PD patients [2]. Accumulating evidence suggests that neurotoxins (MPTP, rotenone and 6-OHDA), aggregation of α-synuclein, genetic mutations (A53T), oxidative stress and bacterial toxins (LPS) can activate the NLRP3 inflammasome, and thus trigger caspase1 activation and caspase1-mediated release of IL1β and IL18, which may lead to the death of dopaminergic neurons in the SNc [2, 29-32]. The NLRP3 inflammasome is a multiprotein complex that acts as intracellular sensors of environmental and cellular

stress, which is composed of NLRP3, apoptosis associated speck-like protein containing a caspase recruitment domain (ASC) and the caspase1 protease [2]. The activation of NLRP3 promotes the secretion of IL1β and thus induces pyroptosis [33]. Pyroptosis is a type of programmed cell death which plays critical roles in maintaining cellular homeostasis. The activation of pyroptosis can further induce the release of IL1β to promote the inflammatory response, which may contribute to PD pathogenesis. Recently, it's reported that DDO7263, a novel Nrf2 activator targeting brain tissue, can protect against MPTP-induced PD model via inhibition of the NLRP3 inflammasome and oxidative stress [34]. Astragaloside IV can ameliorate motor deficits and the loss of dopaminergic neuron induced by MPTP through suppression of NLRP3 inflammasome [35]. Besides, previous studies have revealed that celastrol inhibits microglial pyroptosis and attenuates inflammatory reaction in acute spinal cord injury rats [36]. Besides, celastrol can significantly reduce the secretion of IL1β and IL18 by inhibiting both NLRP3 expression and cleavage of caspase1 in LPS/ATP-activated macrophages [37]. These observations suggest that celastrol could activate Nrf2 and suppress NLRP3 to protect against neuroinflammation. However, whether the celastrol inhibits NLRP3 inflammasome through activation of Nrf2 to exert neuroprotective roles in PD is not yet known.

Accumulating evidence suggests that dopaminergic neurons, astrocytes and microglia coordinately participate in the PD progression [38-40]. It's reported that berberine can protect against 6-OHDA-induced neurotoxicity in human dopaminergic neurons via the induction of Nrf2 [27]. β-lapachone can exert neuroprotective effect in MPTP-induced PD mice via the activation of Nrf2/HO-1 signaling pathway in astrocytes [41]. Activation of dopamine D2 receptor (Drd2) can restrict astrocytic NLRP3 inflammasome activation by enhancing the interaction of β-arrestin2 and NLRP3 [42]. Achyranthes bidentata polypeptide k suppresses neuroinflammation in BV2 microglia through Nrf2-dependent mechanism [43]. Studies report that oral administration of MCC950 can inhibit the NLRP3 inflammasome and thus mitigate motor deficits, loss of dopaminergic neurons and α-synuclein aggregation in multiple rodent PD models [2]. Histologic studies have observed elevated NLRP3 expression in mesencephalic neurons of PD patients, and revealed a rare NLRP3 polymorphism associated with decreased risk of PD [44]. As reported, celastrol mitigates the reactive astrocytes and microglia mediated neuroinflammation to protect dopaminergic neurons against MPTP-induced neurotoxicity [15, 45]. Hence, to investigate the mechanism underlying the neuroprotective actions of celastrol, we next assessed the effects of celastrol on neurons, astrocytes and microglia by immunofluorescence staining approach.

To assess the neuroprotective actions of celastrol in PD, we employed multiple PD models to better understand the nigro-striatal degeneration, including MPTP-induced PD mouse model and the AAV-mediated human α-syn overexpression PD model. By using immunofluorescence technology and genomewide RNA-sequencing approach, we further determined that the inhibition of NLRP3 and the activation of Nrf2 by celastrol may be the potential therapeutic strategy for the treatment of PD. Employment of the genetically modified mice (Nrf2-KO, NLRP3-KO and Caspase1-KO mice) enabled us to conclude that Nrf2 and NLRP3 may play a key role in the neuroprotective effects of celastrol. Taken together, we provide herein direct evidence that celastrol protects against loss of dopaminergic neurons, maintains nigro-striatal system function, and mitigates neuroinflammation through inhibition of NLRP3

inflammasome mediated by Nrf2, suggesting that NLRP3 activation might be a key pathological factor that drives PD pathogenesis and the NLRP3 inhibition by the Nrf2 anti-oxidative pathway may underlie the neuroprotective role of celastrol in PD, which renders celastrol as a promising disease-modifying agents to alleviate progressive dopaminergic degeneration.

Methods And Materials

Mice.

C57BL/6 mice were purchased from Charles River Laboratories. Male mice were used for all the experiments at 8-10 weeks of age described in this study. We maintained mice on a 12 h light-dark cycle in a temperature-controlled high barrier facility with unrestricted access to food and water. During all procedures of experiments, the number of animals and their suffering by treatments were minimized.

Administration of celastrol.

Eight to ten weeks old male mice weighing 24 to 28 g were housed under standard conditions. After 1 week acclimatization, mice were injected with MPTP at a dose of 30 mg/kg i.p. for 5 days, as used previously [46], and the controls were administered an equal volume of saline (0.9 % NaCl). Then mice were administered celastrol (BOC Science Shirley, NY) at dose of 1, 10, 100, 1000 μg/kg for 7, 14, 21 days. Celastrol was dissolved in DMSO (25 μl) and administered to the mice intraperitoneally once a day, as previously reported[2]. All treatments were performed within 90 min before dark cycle and mice received celastrol or vehicle daily.

Reagents

The following primary antibodies have been used in this work: rabbit α-synuclein (Abcam, ab138501),mouse p-α-ynuclein^{Ser129} (Biolegend, 825701), mouse Tyrosine Hydroxylase (TH) (Millipore, AB152), rabbit Tyrosine Hydroxylase (TH) (Santa Crus, sc-25269), rabbit Dopamine transporter (DAT) (Bioss, bs-1714R),rabbit Nrf2 (Abcam, ab31163), mouse Nrf2 (Snata Cruz, sc-365949), rabbit GFAP (Bioss, bs-0199R), mouse GFAP (Snata Cruz, sc-33673), rabbit Iba1 (Wako, 019-19741), mouse Iba1 (GeneTex, GTX632426-S), rabbit NLRP3 (CST, 13158S), rabbit p20 caspase1 (Bioss, bs-10442R), rabbit ASC (Bioss, bs-6741R), rabbit IL1β (Bioss, bs-6319R) and β-actin (Abcam, ab7817). Anti-rabbit IgG / Alexa Fluor 488 were from Bioss (bs-02950-AF488,). Tranzol up, TransScript one-step gDNA removel and cDNA synthesis Super MiX, TransStart Top Green qPCR Super Mix were purchased from TransGen Biotech. RNaseZapTM were obtained from Invitrogen. Triglycerides (TG), Cholesterol (CHO). Celastrol were purchased from BOC Science (Shirley, NY), this compound was used as previously described[2]. Dimethyl sulfoxide (DMSO) were obtained from Amresco (Solon, CA).

Immunohistochemistry and immunofluorescence.

Immunohistochemistry and immunofluorescence were performed on 30-μm thick serial brain sections. Primary antibodies and working dilutions are detailed in Table S1. Mice were perfused with PBS and 4% PFA and brains were removed, followed by fixation in 4% PFA overnight and transfer to 20 % - 30 % gradient sucrose for cryoprotection, and subsequently freezed in OCT compound (Sakura FineTech, Tokyo). For histological studies, brain slices s were blocked with 10% goat serum in PBS with 0.2% Triton X-100 and incubated with TH, GFAP or Iba1 antibodies. After washing with PBS three times, brain tissues were used appropriate biotin secondary antibody, followed by avidin-biotin complex (Zsbio, SP-9001) and visualized with 3,3’-diaminobenzidine (DAB) peroxidase substrate (Zsbio, ZLI-9018). Sections were counterstained with Nissl staining solution (Beyotime, C0117), and photographed by light microscope (Leica DMI 4000B, Wetzlar, Germany). The number of TH- and Nissl-positive dopaminergic neurons, and the number of microglia and astrocytes in the SNpc region, and the density of TH positive fibers in the STR were measured with ImageJ software. For immunofluorescent studies, dual-antigen immunofluorescence was performed to detect the expression level of Nrf2, NLRP3 and Caspase1 in dopaminergic neurons, astrocytes or microglia (TH, GFAP and Iba1). Sections were washed in PBS and incubated with a mixture of Alexa-fluor 488- and 594- conjugated secondary antibodies (1:500, YEASEN) at room temperature for 120 min. Sections were mounted with VectaShield medium (Vector Laboratories) and analyzed by detecting fluorescin using a fluorescence microscope (Leica DMI 4000B, Wetzlar, Germany).The selected area in the signal intensity range of the threshold was measured using ImageJ software.

Total protein extraction and western analysis.

SNc and STR were homogenized with a Polytron in ice-cold RIPA buffer [1% Trinton X 100; 10 mM Na2HPO4 (Sodium phosphate); 150 mM NaCl (Sodium chloride); 1% DOC (Sodium deoxycholate or deoxycholic acid); 5 mM EDTA; 5 mM NaF (sodium Fluoride); 0.1 % SDS] supplemented with protease and phosphatase inhibitors (catalog #P8340 and #P2850; Sigma), sonicated and cleared by centrifugation (10,000 × g, 10 min, at 4 °C). Western procedure was previously described [47]. Protein concentration in the supernatant was determined by BCA assay (Aidlab; PP01). Protein (5 μg) in 1 × sample buffer [62.5 mM Tris•Cl (pH 6.8), 2% (wt/vol) SDS, 5% glycerol, 0.05% (wt/vol) bromophenol blue] was denatured by boiling at 100ºC for 5 min and separated on 8% sodium dodecyl sulfate poly acrylamide (SDS-PAGE) gels and transferred onto nitrocellulose membrane (Pall Corporation; T60327) by electrophoresis. Blots were blocked in 5% nonfat milk in Tris-buffered saline and Tween 20 (TBST) for 2 h at room temperature and probed with primary antibody in 5% BSA-TSBT overnight at 4°C. After overnight incubation, the blots were washed three times in TBST for 15 min, followed by incubation with HRP-conjugated secondary antibody in TBST with 5% nonfat milk for 2 h at room temperature. Following three cycles of 15 min washes with TBST, the blots were developed using an Enhanced Chemiluminescence assay (BIO-Rad). Densitometry analysis was performed on scanned western blot images using the ImageJ software (NIH).

Behavioral tests.

To evaluate the beneficial effect of celastrol on behavioral deficits in MPTP-induced PD mouse model and AAV vectors-mediated human α-syn overexpression induced PD model, mice were assessed by beam traversal, pole test, rotarod test, hindlimb reflect scoring and gait test. Before pharmacological testing, mice were handled for a week by the same operator to reduce stress, and trained for behavioral tests as described below until their motor performance became reproducible. Motor function for all animals was tested between 10:00-16:00 in the lights-on cycle. All tests were performed similarly to previous studies [48, 49]. Apparatus was cleaned with 75% ethanol after each trial.

Beam traversal.

A 1 m beam was constructed of four segments of 0.25 m in length. Each segment was of thinner widths 3.5 cm, 2.5 cm, 1.5 cm, and 0.5 cm, with 1 cm overhangs placed 1cm below the surface of the beam. The widest segment acted as a loading platform for the animals and the narrowest end placed into home cage. Animals had two days of training to traverse the length of the beam before testing. On the first day of training, animals received 1 trial with the home cage positioned close to the loading platform and guided the animals forward along the narrowing beam. Animals received two more trials with limited or no assistance to encourage forward movement and stability on the beam. On the second day of training, animals had three trials to traverse the beam and generally did not require assistance in forward movement. On the third day, animals were timed over three trials to traverse from the loading platform and to the home cage. Timing began when the animals placed their forelimbs onto the 2.5cm segment and ended when one forelimb reached the home cage.

Pole test.

Mice were acclimatized in the behavioral procedure room for at least 30 min. A 75 cm long pole, 1cm in diameter, wrapped with non-adhesive shelf liner to facilitate the animals grip, was placed into the home cage. Animals received two days of training to descend from the top of the pole and into the home cage. On the test day, animals were placed head-down on the top of the pole and timed to descend back into the home cage. Timing began when the experimenter released the animal and ended when one hind-limb reached the home cage base.

Rotarod test.

Rotarod was performed by placing the mice on an accelerating rod (4 to 40 r.p.m. over the course of a 5-min trial, 3 trials/day, 20-min inter-trial interval, for three days). All animals were trained 3 days before rotarod test. Latency to fall were recorded. Motor test data were presented as the percentage of the mean duration (three trials) on the rotarod compared to the control.

Hindlimb reflect scoring.

Animals were gently lifted upward by the mid-section of the tail and observed over 5-10 s. Animals were assigned a score of 0, 1, 2, 3 based on the extent to which the hindlimbs clasped inward. 0, indicating no clasping, was given to animals that freely moved both their limbs and extended them outward. A score of 1 was assigned to animals which clasped one hindlimb inward for the duration of the restraint or if both legs exhibited partial inward clasping. A score of 2 was given if both legs clasped inward for the majority of the observation, but still exhibited some flexibility. A score of 3 was assigned if animals displayed complete paralysis of hindlimbs that immediately clasped inward and exhibited no signs of flexibility.

Gait test.

The testing apparatus is made of a gray acrylic board (3 mm thick), and consists of a runway (10 cm width, 60 cm length, 12 cm height) with non-slippery white paper and a dark goal box (16 cm width, 10 cm length, 12 cm height). On the first training day, mice were habituated to the apparatus for 2 min, then their forepaws and hindpaws were painted red and black with non-toxic dyes and trained to run to the goal box (training trial). In test trials, mice were made to run the runway in the same manner (cut-off time 60 s maximum). The footprint patterns were analyzed for three parameters (stride length, stride width, and overlap), prints near the start and the goal being excluded because of the effects of acceleration or deceleration. Stride length was measured as the average distance between each forepaw and hindpaw footprint. Stride width was measured as the average distance between the right and left footprint of each forepaw and hindpaw. Overlap was measured as the average distance between the center of forepaw and hindpaw footprints on the same side. At least four values were measured in each trial for each parameter.

Quantitative real-time PCR.

Total RNA was extracted from adipose tissues and hypothalamus using TRIzol reagent (TransGen Biotech). Quantification and integrity analysis of total RNA was performed by running 1 μl of each sample on NanoDrop 5500 (Thermo). The cDNA was prepared by reverse transcription (TransScript one-step gDNA removel and cDNA synthesis Super MiX, TransGen Biotech). The relative expression of mRNAs was determined by the SYBR Green PCR system (Bio-Rad). The relative expression of genes of interest was calculated by comparative Ct method and GAPDH was used as an endogenous control. GAPDH RNA was chosen as the housekeeping gene. Sequences of the primers used for real-time qPCR are available in table S1: Primers used in the present study.

Table S1: Primers used in this study.

Primer	Forward Primer 5'-3'	Reverse Primer 5'-3'
TNF-a	GACGTGGAACTGGCAGAAGAG	TTGGTGGTTTGTGAGTGTGAG
IL-1beta	GAAATGCCACCTTTTGACAGTG	TGGATGCTCTCATCAGGACAG
IL-6	TAGTCCTCCTACCCCAATT	TTGGTCCTTAGCCACTCCTT
IL-8	CTTACTGACTGGCATGAGGATCA	GCAGCTCTAGGAGCATGTGG
NF-kB	AGAGGGGATTTCGATTCCGC	CCTGTGGGTAGGATTTCTTGTTC
iNOS	AAGTCGGGGAGGAGTTTCACG	GGAGCTTAACGGAGGCTTGGA
GFAP	CGGAGACGCATCACCTCTG	TGGAGGAGTCATTCGAGACAA
Iba-1	CTTGAAGCGAATGCTGGAGAA	GGCAGCTCGGAGATAGCTTT
PGC1a	TCCACTGTCCACCTGATTGA	TGGCATGTAGTCTGGAGCTG
UCP2	ATATAAGCCCAACTGCAGGAAA	GTCAAAGTCAGTGCGTTCAAAG
MFN1	CCGGTCGATGCAACGAGTGATGAGG	GCCTCCAGCTTGCATGATCTCCGG
MFN2	TACGAAGTGGTCTGTGGGCAATCA	TCAGCTTGTTGGACAGGGCTATCA
Drp1	CCACAGGACAGTACAGGATG	TCAAGTCGTGCTGAATAATACC
OPA1	ATGGTGAAGCTGATCGAGAGC	GGCATA TTCAGTAATAGAGGC
PINK1	CGCCTATGAAATCTTTGGGC	GCACTGCCTTGGCCATAGAA
Tfam	AAAAGTCGGGGTCTCTCTGAC	CAGTCGGTCCAAAATTCTTGTGA
Nrf1	GGACCCAGTCAGGTTGGTG	TCCTGGTCTAAGCCGATTATCAT
Fis1	ATGTGGCACTTTTATGTGACCA	CCCCAGGTTCTTGTCGTCTTG
Bcl-2	CCTGTGGATGACTGAGTACC	CCCACTCGTAGCCCCTCT
Bcl-xl	TGCCCAAGCTCAACTTGAAGA	TGGCCGTAGACGGTTGTCATA
Bax	GGCGAATTGGAGATGAAC	CCGAAGTAGGAGAGGAGG
Caspase3	CCCCTGTCATCTTTTGTCCCT	AGCTGGCAGAATAGCTTATTGAG
Caspase9	GGCTGTTAAACCCCTAGACCA	TGACGGGTCCAGCTTCACTA
PUMA	CATGGGACTCCTCCCCTTAC	CACCTAGTTGGGCTCCATTT
CHOP	AAGCCTGGTATGAGGATCTGC	TTCCTGGGGATGAGATATAGGTG
ATF6	TCGCCTTTTAGTCCGGTTCTT	GGCTCCATAGGTCTGACTCC
GRP78	ACTTGGGGACCACCTATTCCT	GTTGCCCTGATCGTTGGCTA
XBP1	AGCTTTTACGGGAGAAAACTCAC	CCTCTGGAACCTCGTCAGGA

ERN1	ACACTGCCTGAGACCTTGTTG	GGAGCCCGTCCTCTTGCTA
Nrf2	TTCTTTCAGCAGCATCCTCTCCAC	ACAGCCTTCAATAGTCCCGTCCAG
HO-1	CAAGCCGAGAATGCTGAGTTCATG	GCAAGGGATGATTTCCTGCCAG
NQO1	GCGAGAAGAGCCCTGATTGTACTG	TCTCAAACCAGCCTTTCAGAATGG
GCLC	ACATCTACCACGCAGTCAAGGACC	CTCAAGAACATCGCCTCCATTCAG
GCLM	GCCACCAGATTTGACTGCCTTTG	TGCTCTTCACGATGACCGAGTACC
Gapdh	AGGTCGGTGTGAACGGATTTG	TGTAGACCATGTAGTTGAGGTCA

Whole-genome sequencing analysis.

Total RNA was extracted from SNc using TRIzol reagent (TransGen Biotech). Quantification and integrity analysis of total RNA was performed by running 1 μl of each sample on NanoDrop 5500 (Thermo). A total amount of 3 μg RNA per sample was used as input material for the RNA sample preparations. After that, the RNAs were subjected to 50-bp single-end sequencing with a BGISEQ-500 sequencer as previously described [50]. At least 20 million clean reads of sequencing depth were obtained for each sample. Differential expression analysis of two groups (two biological replicates per condition) was performed using the DESeq R package (1.10.1). DESeq provide statistical routines for determining differential expression in digital gene expression data using a model based on the negative binomial distribution. The resulting P-values were adjusted using the Benjamini and Hochberg's approach for controlling the false discovery rate. Genes with an adjusted P-value <0.05 found by DESeq were assigned as differentially expressed. DEGs were defined as genes with FDR less than 0.01 and log2 fold change larger than 1 (upregulation) or smaller than -1 (downregulation). Gene Ontology (GO) and pathway annotation and enrichment analyses were based on the NCBI COG (https://www.ncbi.nlm.nih.gov/COG/), Gene Ontology Database (http://www.geneontology.org/) and KEGG pathway database (http://www.genome.jp/kegg/), respectively. The software Cluster and Java Treeview were used for hierarchical cluster analysis of gene expression patterns.

Adeno-associated virus induced overexpression of human alpha-synuclein.

Recombinant AAVs (serotype 2 genome packaged in serotype 9 capsid) were used for the expression of human wild-type α-syn, GFP driven by the human synapsin-1 promoter and enhanced using a woodchuck hepatitis virus posttranscriptional regulatory element (WPRE) [51, 52].

Stereotaxic injection.

Vector solution was bilaterally injected within the SNc region using a 0.2 mm-gauge stainless steel injector connected to a 5 μl Hamilton syringe. In all experimental groups, the AAV was injected in a volume of 1 μl / side at a rate of 0.2 μl / min. The stereotaxic coordinates used (flat skull position) were: AP = −3.2 mm; ML = ± 1.2 mm, DV = −4.6 mm relative to the bregma, according to the atlas of Paxinos and Franklin (2001). Only animals with correct injection placements, verified by analysing immunofluorescence staining of consecutive coronal brain sections, were included in the statistical analysis transgene expression of human wild type alpha-synuclein.

Sample collection and tissue preparation.

For collecting feces, mice were placed individually in empty autoclaved cages and allowed to defecate freely in the morning after the day of last treatment. Once feces were formed of each mouse, they were collected immediately in individual sterile EP tubes into liquid nitrogen and then stored at −80 °C until next usage.

Statistical analysis.

Data are expressed as the mean ± s.e.m. with at least three biologically independent experiments. Representative morphological images were taken from at least three biologically independent experiments with similar results. Statistical significance was determined using an unpaired two-tailed Student t-test or a two-way ANOVAs followed by Tukey's multiple comparisons test were used. All data were analyzed using the appropriate statistical analysis methods, as specified in the figure legends, with the SPSS software (version 19.0). The test was performed using SPSS. Significance was accepted at * $P < 0.05$, ** $P < 0.01$ or *** $P < 0.001$.

Results

Celastrol protects against loss of dopaminergic neurons in MPTP-induced PD mice

To assess the neuroprotective potential of celastrol in PD, the MPTP-induced PD mouse model was firstly employed. It's reported that celastrol may exert biphasic effect on neuroprotective properties, that is, celastrol at the low doses protects against the neurotoxicity; while celastrol at the high doses exacerbates the neurotoxicity [53]. Therefore, to gain the desired therapeutic outcome of celastrol with high efficiency and low toxicity, we examined a range of dosages (Supplementary Fig. 1-3) and treatment course (Supplementary Fig. 4-6). We found that celastrol treatment at the doses of 10, 100 and 1000 μg/kg relieved the reduction in tyrosine hydroxylase (TH) immunoreactivity in the SNc and STR (Supplementary

Fig. 1b, Supplementary Fig. 2a), mitigated the impaired motor function (Supplementary Fig. 1d), attenuated the loss of dopaminergic neurons and led to a greater TH^+ fibers density in the STR (Supplementary Fig.3) in response to MPTP injection, as compared with controls. Besides, celastrol administration at the doses of 10 μg/kg in treatment courses for 7, 14, 21 days showed significant neuroprotective actions against MPTP injection (Supplementary Fig. 4a,c, Supplementary Fig.5b, Supplementary Fig. 6). We also observed that celastrol alone had no obvious effect on the number of dopaminergic neurons in the SNc, the TH^+ fibers density in the STR and motor function (Supplementary Fig. 1c, e, Supplementary Fig. 2b, Supplementary Fig. 4b, d, and Supplementary Fig. 5a). Based on these observations, we decided to initiate treatment with celastrol (10 μg/kg) for 7 days in MPTP-induced PD mouse model to explore the mechanism underlying the neuroprotective role of celastrol, as shown in Fig. 1a.

Celastrol treatment led to marked restoration of the loss of dopaminergic neurons (~70 % *vs.* 48 %, $P < 0.01$) (Fig. 1b), the reduction of TH protein levels in the SNc (~66 % *vs.* 47 %, $P < 0.001$) (Fig. 1c) and STR (70 % *vs.* 48 %, $P < 0.05$) (Supplementary Fig. 8b), under the condition of MPTP injection, compared with controls. The decrease of TH^+ fibers density (~74 % *vs.* 50 %, $P < 0.01$) in response to MPTP injection was also mitigated by Celastrol treatment (Supplementary Fig. 8a). Besides, pole descent, rotarod test, beam traversal, hindlimb clasping reflexes, and gait test showed that the impairment of motor coordination and balance were relieved by celastrol treatment (Fig. 1d, e). Together, these results suggest that celastrol treatment alleviates the dopamine synthesis, maintains the nigrostriatal function and attenuates the motor function. Given that celastrol exhibits profound anti-neuroinflammatory effects [13, 14], the mitigatory effect of celastrol on neuroinflammation triggered by MPTP injection was further assessed. We observed that celastrol treatment led to a significantly decreased number of $GFAP^+$ (glial fibrillary acidic protein) and $Iba1^+$ (ionized calcium-binding adapter molecule 1) cells, as well as GFAP and Iba1 protein levels in the both SNc and STR (Supplementary Fig. 9a-c), suggesting that celastrol may mitigate reactive glia cells-mediated neuroinflammation. Similarly, quantitative PCR analysis showed that celastrol treatment suppressed genes associated with pro-inflammatory (*TNFα, IL1, IL6*) and activated genes linked to anti-inflammatory (*IL4, IL10*) (Fig. 1f). Besides, celastrol treatment led to mitigation of genes related to anti-oxidative stress (*Nrf2, HO1, NQO1, GCLC* and *GCLM*), mitochondrial function (*Pgc1α, Ucp2, Drp1 and Mfn1*); normalized genes linked to apoptosis (*Caspase3 and Caspase9*) and ER stress (*CHOP, GRP78, ERN1, Xbp1* and *ATF6*) (Fig. 1f), highlighting the multiple bioactivities of celastrol in PD. Taken together, these results demonstrate that celastrol can mitigate the MPTP-induced PD-like symptoms, rendering celastrol as a promising disease-modifying agents of PD.

Nrf2, NLRP3 and Caspase1 are identified as therapeutic targets of celastrol

To explore the mechanism underlying the neuroprotective action of celastrol in PD, whole-genome RNA-sequencing analysis was performed to identify differential expression genes (DEGs) in the SNc of MPTP-

induced PD mice treated with celastrol. Gene expression profiles (Fig. 2a) and DEGs (Fig. 2b) were visualized as heatmap respectively. Celastrol treatment mitigated the genes linked to locomotory behavior (*TH, SLC6A3, Nr4a2, Drd2* and *Trpc2*); anti-oxidative stress (*Nfe2l2, Hmox1, Nqo1, Sod2, Gpx1*); autophagy-lysosomal pathway (*Beclin1, Ern1* and *Hspa5*) and ubiquitin-proteasome system (*Usp14, Alfy, Hsp70*) under the condition of MPTP treatment (Fig. 2a,b). Celastrol led to a significant decrease of genes associated with neuroinflammation (*Gfap, Aif1, Nlrp3, IL18, ASC*); apoptosis (*Bcl2, Bax, Nlrp1a*) and ER stress (*Ddit3, Ern1, Hspa5, Xbp1*) (Fig. 2a, b). To obtain deeper insights into signaling pathways regulated by celastrol, GO (gene ontogeny) and KEGG (Kyoto Encyclopedia of Genes and Genomes) analyses of DEGs were performed. We observed that celastrol treatment led to a marked increase in pathways related to locomotory behavior, dopamine neuron differentiation, neuronal signal transduction and neurotransmitter transport; while celastrol inhibited pathways associated with inflammation, apoptotic process and neuron death (Fig. 2c, d). Further, volcano plot and Venn diagram showed that celastrol treatment led to an induction of *TH, SLC6A3, Nfe2l2, Homx1* and *NQO1*, and a decrease *of GFAP, AIF1, NLRP3, ASC, Caspase1* and *ASC* in response to MPTP injection (Fig. 2e, f). Nrf2 (NFE2L2) is a critical transcription factor in anti-oxidative and anti-neuroinflammatory process in PD progression [22, 54]. It's recently reported that the activation of NLRP3-mediated inflammasome is a newly discovered pathogenesis of PD, which triggers caspase1 activation and caspase1-mediated release of IL1β and IL18, and this activation finally drives progressive dopaminergic neuropathology [2, 29, 30]. By using STRING database, Nrf2, NLRP3 and Caspase1 proteins and their functional interactions which formed the backbone of the cellular machinery were exhibited (Fig. 2g). Gene network analysis showed that the *Nrf2, HO1, NQO1* mRNA levels were positively correlated with TH mRNA levels, while *NLRP3, ASC* and *IL1β* mRNA levels were negatively correlated with *TH* mRNA levels in the human SNc, suggesting that *Nrf2, HO1, NQO1* may underlie the neuroprotective effects of celastrol in PD, and *NLRP3, ASC* and *IL1β* may contribute to PD pathogenesis (Fig. 2k). Taken together, these results suggest that Nrf2, NLRP3 and Caspase1 may be critical factors that underlie the pleiotropic effects of celastrol in PD treatment.

The neuroprotective effects of celastrol against PD is Nrf2-dependent

As we have already demonstrated that celastrol treatment led to a significant increase in Nrf2 levels in response to MPTP injection (Fig. 2), hence, to further determine whether Nrf2 mediates the neuroprotective effects of celastrol, Nrf2-KO mice were employed. As previously reported, deficiency of Nrf2 caused a more profound loss of dopaminergic neurons in the SNc (Fig. 4a) [55], and celastrol treatment failed to restore the loss of dopaminergic neurons and the decrease in TH^+ fibers density in the Nrf2-KO mice under the condition of MPTP (Fig. 4a). Likewise, the neuroprotective effect of celastrol on the reduced TH and DAT protein levels by MPTP was impeded in Nrf2-KO mice when compared with controls (Fig. 4c). Besides, celastrol treatment failed to restore the impairment of motor coordination and balance induced by MPTP in Nrf2-KO mice (Fig. 4d). Collectively, these results suggest that Nrf2 may mediate the beneficial effects of celastrol against PD. It's reported that Nrf2 signaling involves the anti-

neuroinflammatory effect of fumaric acid in MPTP-induced PD mice [54]. Therefore, we further investigated whether Nrf2 could be linked to the anti-neuroinflammatory action of celastrol in PD. We observed that mitigative effect of celastrol treatment on the activation of $GFAP^+$ astrocytes and $Iba1^+$ microglia was halted in the SNc of MPTP administrated Nrf2-KO mice (Supplementary Fig. 10). These results suggest that celastrol exerts anti-neuroinflammatory effect via the activation of Nrf2, which may contribute to the neuroprotective role of celastrol in PD.

It is well established that activation of Nrf2 can exhibit the beneficial effects on PD in neurons, astrocytes, and microglia [20, 56]. Hence, to better understand the mechanism underlying the neuroprotective properties of celastrol, we next asked in which cell types Nrf2 participates in the actions of celastrol. By using double staining of Nrf2 with cell-types specific markers (TH for dopaminergic neurons, GFAP for astrocytes and Iba1 for microglia) within SNc, we found that celastrol treatment normalized Nrf2 level under the condition of MPTP predominantly in dopaminergic neurons, while celastrol treatment had little effect on Nrf2 level in both astrocytes and microglia (Supplementary Fig. 11 and Supplementary Fig. 12). Taken together, these findings suggest that Nrf2 may mediate the neuroprotective and anti-neuroinflammatory actions of celastrol mainly in dopaminergic neurons.

Celastrol inhibits NLRP3 inflammasome to protect against PD via activation of Nrf2

Given that NLRP3 inflammasome have been observed in the SNc of both PD patients and PD animal models [2], hence, to confirm whether NLRP3 is involved in the effect of celastrol in PD, the NLRP3-KO mice were employed. As previously reported, the activation of NLRP3 and ASC triggered by MPTP injection were testified by western and immunohistochemistry analysis (Supplementary Fig. 7) [32, 57]. We found that the loss of dopaminergic neurons in the SNc and the decrease in density of TH^+ fibers in the STR (Fig. 4a) were relieved in MPTP treated NLRP3-KO mice. The reduction in TH and DAT protein levels in the both SNc and STR (Fig. 4c) and the impairment of motor function (Fig. 4b, d) were mitigated in MPTP treated NLRP3-KO mice, while the neuroprotective effect of celastrol was lost in MPTP treated NLRP3-KO mice (Fig. 4a-d). These results suggest that NLRP3 may underlie the neuroprotective action of celastrol in PD. Besides, we observed that activation of astrocytes and microglia in the both SNc and STR induced by MPTP was ameliorated in NLRP3-KO mice, while celastrol treatment led to a slight but not significantly higher anti-inflammatory effect (Supplementary Fig. 13), suggesting that NLRP3 may mediate the anti-neuroinflammatory action of celastrol in MPTP-induced PD mice.

The effects of celastrol are mediated by Nrf2-NLRP3-Caspase1 axis

It's recently reported that Caspase1 deficiency alleviates the loss of dopaminergic neurons in MPTP-induced PD [58]. To determine whether Caspase1 underpins the neuroprotective action of celastrol in PD,

the Caspase1-KO mice were applied. We found that the Caspase1 deficiency led to profound restoration of the loss of dopaminergic neurons in the SNc (Fig. 5a), the reduction of TH^+ fibers in the STR (Fig. 5a), the decrease of TH and DAT levels in the both SNc and STR (Fig. 5c), as well as the deficit of motor function (Fig. 5b, d); while the neuroprotective actions of celastrol were lost (Fig. 5a-d) in Caspase1-KO mice compared with controls. These findings demonstrate that the neuroprotective effects of celastrol in PD may be mediated by the inhibition of Caspase1, which also confirm that Caspase1 may be a potential therapeutic target of PD treatment. Since Caspase1 is associated with neuroinflammation during PD progression [59], we further decided to ascertain the role of Caspase1 in the anti-neuroinflammatory action of celastrol. As shown in Supplementary Fig. 14, the increased number of $GFAP^+$ and $Iba1^+$ cells in the both SNc and STR was mitigated by celastrol treatment; while celastrol treatment lost mitigative effect on activation of astrocytes and microglia in Caspase1-KO mice compared with controls, suggesting that the inhibition of Caspase1 contributes to the neuroinflammatory effect of celastrol.

Accumulating evidence suggests that the activation of NLRP3 inflammasome has been found in both microglia and dopaminergic neurons of PD patients SNc [2, 30, 32, 58, 60]. Hence, to investigate in which cell types NLRP3 inflammasome acts on, the Co-labelling analysis of ASC with TH, GFAP and Iba1 was manipulated. We observed that celastrol treatment led to a profound decrease of ASC levels triggered by MPTP in dopaminergic neurons, microglia and astrocytes (Supplementary Fig. 15 and Supplementary Fig. 16). These results suggest that celastrol may act on dopaminergic neurons and microglia to depress the activation of NLRP3 induced by MPTP.

Notably, we observed that celastrol treatment had little mitigatory effect on the activation of NLRP3 in Nrf2-KO mice (Fig. 6a). It's reported that Nrf2 activator DDO7263 can protect against the MPTP-induced PD like symptom via the inhibition of NLRP2 inflammasome [34]. Therefore, to ask whether the attenuation of NLRP3 by celastrol is dependent on the activation of Nrf2, western analysis was performed. We found that celastrol treatment led to marked induction of Nrf2 and its downstream factors (HO1 and NQO1) in NLRP3-KO mice (Fig. 6b) which suggest that Nrf2 might be the upstream regulator of NLRP3 in the action of celastrol in PD. Taken together, these results demonstrate that celastrol inhibits NLRP3 inflammasome to protect against PD via the activation of Nrf2, suggesting that Nrf2-NLRP3 axis may underlie favorable effects of celastrol in PD treatment.

It's well documented that NLRP3 inflammasome is mainly composed of NLRP3, adaptor ASC and effector molecule Caspase1, which can promote IL1β and IL18 to exacerbate neuroinflammation during PD progression [30, 58]. It is reported that Isoliquiritigenin inhibits Caspase1 via the regulation of Nrf2, which contributes to its neuroprotective and anti-neuroinflammatory effects [61]. We found that celastrol treatment elevated Nrf2 to inhibit NLRP3 levels in Caspase1-KO mice (Fig. 6c), suggesting that Nrf2-NLRP3 axis may be involved in the inhibition of Caspase1 to exert neuroprotective roles in PD. Taken together, these results suggest that the effects of celastrol are mediated by Nrf2-NLRP3-Caspase1 axis.

Celastrol protects against neurodegeneration of dopaminergic neurons in mice overexpressing human α-syn.

As the aggregation of α-syn is the hallmark of PD, to model the neurodegeneration of the dopaminergic neurons, AAV-mediated human wild-type α-syn overexpression within SNc by stereotactic injections was performed, as shown in Fig. 7a. Co-labelling with TH (red) and GFP (green fluorescent protein) ascertained that α-syn predominantly expressed within SNc at 21 days post injection (Fig. 7b). Similar results were observed that human α-syn (h-α-syn) overexpression caused significant loss of dopaminergic neurons in the SNc (Fig. 7c) [52], reduction of TH and DAT protein levels in the SNc (Fig. 7d) and STR (Supplementary Fig.17c), and these changes were markedly rescued by celastrol administration. These results suggest that celastrol protects against the neurodegeneration of the dopaminergic neurons induced by α-syn overexpression. Consistently, behavioral tests showed that the impairment of motor function was also rescued by celastrol treatment (Fig. 7e, f). Besides, α-syn overexpression led to a remarkable increase of $GFAP^+$ and $Iba1^+$ cells, as well as GFAP and Iba1 immunoreactivity in the both SNc and STR (Supplementary Fig. 17a, b), which were mitigated by celastrol treatment (Supplementary Fig. 17a-c). These results suggest that celastrol can relieve the degeneration of the dopaminergic neurons and mitigate neuroinflammation induced by AAV-mediated human wild-type α-syn overexpression, highlighting the multiple neuroprotective properties of celastrol in PD. Given that celastrol treatment led to significant mitigation of genes linked to ALP and UPS function in MPTP-induced PD mice, it's possible that celastrol may alleviate α-syn pathology to impede the dopaminergic neuronal degeneration by enhancement of ALP and UPS function.

As the diagram illustrates in Fig. 6g, our findings suggest that the neuroprotective action of celastrol in PD is mainly dependent on the mitigation of oxidative stress and the relief of NLRP3 inflammasome via Nrf2-NLRP3-Caspase1 axis. Besides, celastrol protects against the neurodegeneration of dopaminergic neurons and the reactive astrocytes and microglia mediated neuroinflammation under the condition of MPTP and human α-synuclein overexpression. Collectively, we demonstrate favorably neuroprotective effects of celastrol which renders it as a promising disease-modifying agent in the treatment of PD.

Discussion

The major findings of this paper are the observation that celastrol protects against the loss of dopaminergic neurons and maintains the nigro-striatal system function, and attenuates the motor deficit in both MPTP-induced and human α-synuclein overexpression-induced PD mouse model. It's well established that the hallmark of PD is the loss of dopaminergic neurons [6, 8, 39, 62, 63]. Recently, the glia (astrocyte and microglia) mediated neuroinflammation has been found to play critical roles in the pathologies of PD [38-40]. It's recently reported that GLP-1 receptor agonists (exenatide, NLY01) may prevent pathological microglial activation and secretion of the proinflammatory cytokines (TNFα, IL1) to prevents the conversion of resting astrocytes to the toxic and reactive A1 phenotype; and Amylin

Pharmaceuticals' and AstraZeneca's GLP-1 receptor agonist exenatide and Novo Nordisk's Liraglutide, Sanofi's Lixisenatide, and Neuraly's NLY-01 are in placebo-controlled phase 2 trial in patients with moderate PD [8, 48, 64]. These reports show that both the dopaminergic and neuroinflammation-targeting therapies may contribute to the development of PD treatments. Notably, a small-molecule NLRP3 inhibitor, MCC950, inhibits NLRP3 inflammasome activation and effectively mitigates motor deficits, nigrostriatal dopaminergic degeneration, and accumulation of α-synuclein aggregates [2]. In this study, we observed that one of the most profound effects of celastrol treatment is the alleviation of the reactive astrocyte and microglia mediated neuroinflammation, and the significant mitigation of genes related to neuroinflammation (*NLRP3, GFAP, Iba1, IL6, IL8, TNFα, IL1*), which may contribute to the neuroprotective action of celastrol in PD. Besides, we also found that celastrol treatment caused remarkable restoration of genes linked to oxidative stress (*Nrf2, HO1, NQO1*), mitochondrial function (*Ucp2*, *Pgc1α*, *Drp1*) and ER stress (*CHOP, GRP78, ERN1*). These findings indicate the multiple biological properties associated with PD treatment, rendering celastrol as a promising candidate in the development of PD treatments.

Nowadays, whole-genome deep sequencing analysis provides the ability to elucidate the underlying pathogenesis of PD, and to dissect the potential target for treatment of PD [65]. By using RNA-sequencing approach, we identified a series of DEGs (*Nrf2, NLRP3, Caspase1*) in SNc of MPTP-induced PD mice treated with celastrol. To obtain deeper insights into signaling pathways regulated by celastrol, GO, KEGG analysis, volcano plot and Venn analysis were performed, we found that celastrol treatment led to a marked increase in pathways related to locomotory behavior, dopamine neuron differentiation, neuronal signal transduction and neurotransmitter transport, while celastrol inhibited pathways associated inflammation, apoptotic process and neuron death. Besides, celastrol treatment led to mitigation of genes related to anti-oxidative stress, mitochondrial function, inhibited genes linked to apoptosis and ER. These findings highlight that celastrol exerts pleiotropic effects to protect against PD.

It is well documented that Nrf2 expresses in neurons, astrocytes and microglia [66]. NLRP3 inflammasome is implicated in the pathogenesis of PD via promoting the death of dopaminergic neurons [2, 29, 30]. It's reported that NLRP3 inflammasome is highly expressed in the microglia of PD patients, and several reports show about the accumulation of NLRP3 inflammasome in dopaminergic neurons of PD patients [29, 31, 58]. Therefore, to further understand the mechanism underlying the effects of celastrol, the co-labelling analysis of Nrf2 and ASC with CNS cell type specific markers (TH, GFAP and Iba1) were performed. We observed that celastrol treatment led to profound activation of Nrf2 in dopaminergic neurons, and inhibition of ASC in both dopaminergic neurons and microglia. It's reported that the inhibition of NLRP3 in microglia by MCC950 can effectively mitigate motor deficits, nigrostriatal dopaminergic degeneration, and accumulation of α-synuclein aggregates [2], while some studies have also shown that dopamine released form dopaminergic neurons can inhibit NLRP3 activation in microglia through the DRD1-CAMP pathway, which suggests that neurons and the NLRP3 inflammasome regulate each other in a bidirectional fashion [33, 67]. These observations suggest that NLRP3 can promote inflammatory reaction to damage dopaminergic neurons, and dopaminergic neurons can also inhibit NLRP3 activation. Thus, we hypothesized that celastrol may act on dopaminergic neurons and microglia to inhibit the activation of NLRP3, which may underlie the neuroprotective roles of celastrol in

PD. To determine whether the neuroprotective effect of celastrol on PD is mediated via the activation of Nrf2, the Nrf2-KO mice were employed. We observed a more profound loss of dopaminergic neurons and impairment of motor function in Nrf2-KO mice under the condition of MPTP compared with controls, which is consistent with previous reported [55]. And celastrol treatment did not caused significant restoration of loss of dopaminergic neurons, impairment of motor function and the neuroinflammation in Nrf2-KO mice, revealing that Nrf2 mediates the neuroprotective effects of celastrol in PD. It's reported that Nrf2/HO-1 mediates the neuroprotective effect of mangiferin by attenuating mitochondria-related apoptosis and NLRP3 induced neuroinflammation; astragaloside IV ameliorates motor deficits and dopaminergic neuron degeneration via inhibiting NLRP3 mediated neuroinflammation and oxidative stress in PD mouse model [35]. Here, our findings show that celastrol treatment protects against the loss of dopaminergic neurons via the mediation of Nrf2-NLRP3 axis in MPTP-induced PD mouse model.

Newly discovered evidence suggests that NLRP3 inflammasome, which occurs in response to neurotoxicity (MPTP, rotenone), misfolded proteins (α-syn) and autophagy defect in the CNS, has emerged as a critical neuroinflammatory mechanism that drives neurodegeneration, rendering it as an important therapeutic target in PD [2, 29, 30, 60]. Among various caspases, caspase1 is a prototypical member, which can be triggered within a molecular platform called inflammasome, is responsible for the production of IL1β and IL18, and these inflammatory cytokines promote the inflammatory response, which may exacerbate PD pathogenesis [58]. Recently, NLRP3-caspase1 axis has emerged as promising therapeutic targets of neurodegenerative diseases, like Parkinson's disease and Alzheimer's disease [68]. In this study, our findings reveal that celastrol treatment suppresses the activation of NLRP3 and Caspase1 in MPTP-induced PD mice. And these two factors are mainly compositions of NLRP3 inflammasome. By using NLRP3-KO and Caspase1-KO mice, we further observed that both NLRP3 and Caspase1 deficiency exhibited profound mitigation of the loss of dopaminergic neurons, nigro-striatal function, the neuroinflammation and motor function in MPTP-induced PD mice. Moreover, we demonstrate that NLRP3-caspase1 axis mediated the beneficial effects of celastrol in PD.

Parkinson's disease is classified as a synucleinopathy, as α-syn, is a major constituent of Lewy bodies and Lewy neurites within dopaminergic neurons [63, 69]. There is growing evidence suggests that α-syn plays central role in the etiology of PD [40], as it links familial and sporadic forms of PD. Hence, to model the neurodegeneration of PD and to ascertain the neuroprotective roles of celastrol in PD, the AAV vectors-mediated human wild-type α-syn overexpression within the SNc was employed, which is considered as useful approach for preclinical validation of new therapeutic agents [40, 63, 70]. Here, our findings demonstrate that celastrol treatment protects against the neurodegeneration of dopaminergic neurons and nigro-striatal system, and mitigates the impairment of motor function. As previously reported, celastrol protects human neuroblastoma SH-SY5Y cells from rotenone-induced injury through induction of autophagy [12]; we confirmed that celastrol treatment led to a profound induction of genes associated with ALP and UPS functions. And this result suggests that promotion of ALP and UPS is implicated in the neuroprotective effects of celastrol in PD.

Conclusions

To date, there's no disease-modifying agents for the treatment of PD [8], and recent genetic gene therapies failed to show favorable anti-neurodegenerative effect [9]. Therefore, development of the neuroprotective agents to halt, delay or prevent the progression of PD remains a high priority. In this study, our work suggest that celastrol protects against the loss of dopaminergic neurons, maintains nigro-striatal system function, mitigates neuroinflammation and ameliorates motor defect via the mediation of Nrf2-NLRP3-Caspase1 axis, suggesting broad neuroprotective properties of celastrol, which render it as a promising candidates of PD treatment, and may help to improve the understanding of PD pathogenesis.

Abbreviations

AAV: Adeno-associated virus; MPTP: 1-methyl-4-phenyl-1,2,3,6-tetrahydropyridine; GFAP: glial fibrillary acidic protein; ASC: Apoptosis-associated speck-like protein containing a CARD; Nrf2: Nuclear factor (erythroid-derived 2)-like 2; Iba-1: Ionized calciumbinding adapter molecule 1; IL-4: Interleukin-4; NFκB: Nuclear factor kappa-light-chainenhancer of activated B cells; NLRP3: NOD- LRR- and pyrin domaincontaining 3; PD: Parkinson's disease; RNAseq: RNA sequencing; SNc: Substantia nigra pars compacta; TH: Tyrosine hydroxylase; DAT: Dopamine transporter; TNF-α: Tumor necrosis factor-α; α-syn: Alpha-synuclein.

Declarations

Ethics approval and consent to participate

Not applicable.

Consent for publication

Not applicable.

Availability of data and materials

The datasets used and/or analyzed during the current study are included in this article and its supplementary information files. The datasets are available from the corresponding author on reasonable request.

Competing interests

The authors declare no competing financial interests.

Funding

This work was supported by grants from the National Natural Science Foundation of China (No.81471064, No. 81670779 and No. 81870590 to R.Z), the Beijing Municipal Natural Science Foundation (No. 7162097 and No. H2018206641 to R.Z), and the Peking University Research Foundation (No. BMU20140366 to R.Z), and the National Key Research and Development Program of China (2017YFC1700402 to R.Z.).

Author contribution

C.Z. and M.Z. did the experiment, analyzed the data. B.W., J.S., and B.G. participated in experiments. M.Z. and R.Z. wrote the manuscript. R.Z. conceived the idea of study and manuscript writing. All authors reviewed and approved the manuscript for submission.

Acknowledgement

We thank Siwang Yu (School of Pharmaceutical Sciences, Peking University Health Science Center) for providing Nrf2-KO mice; Han Xiao (Peking University Third Hospital) for providing NLRP3 KO mice, Changtao Jiang (Peking University Health Science Center) for providing Caspase1-KO mice.

We thank K. Wang (Histology Facility of Department of Anatomy, Histology and Embryology, Peking University) for technical support. We also thank S. Zhu (Department of Physiology and Pathophysiology, Peking University) and M. Ye (Peking University School of Pharmaceutical Sciences) for providing access to necessary equipments.

References

1. Tan EK, Chao YX, West A, Chan LL, Poewe W, Jankovic J: Parkinson disease and the immune system - associations, mechanisms and therapeutics. Nat Rev Neurol. 2020.
2. Gordon R, Albornoz EA, Christie DC, Langley MR, Kumar V, Mantovani S, et al: Inflammasome inhibition prevents alpha-synuclein pathology and dopaminergic neurodegeneration in mice. Sci Transl Med. 2018; 10.
3. Matheoud D, Cannon T, Voisin A, Penttinen AM, Ramet L, Fahmy AM, et al: Intestinal infection triggers Parkinson's disease-like symptoms in Pink1(-/-) mice. Nature. 2019; 571:565-569.
4. Shahnawaz M, Mukherjee A, Pritzkow S, Mendez N, Rabadia P, Liu X, et al: Discriminating alpha-synuclein strains in Parkinson's disease and multiple system atrophy. Nature. 2020; 578:273-277.
5. Klingelhoefer L, Reichmann H: Pathogenesis of Parkinson disease--the gut-brain axis and environmental factors. Nat Rev Neurol. 2015; 11:625-636.

6. Johnson ME, Stecher B, Labrie V, Brundin L, Brundin P: Triggers, Facilitators, and Aggravators: Redefining Parkinson's Disease Pathogenesis. Trends Neurosci. 2019; 42:4-13.
7. Barker RA, consortium T: Designing stem-cell-based dopamine cell replacement trials for Parkinson's disease. Nat Med. 2019; 25:1045-1053; Verschuur CVM, Suwijn SR, Boel JA, Post B, Bloem BR, van Hilten JJ, et al: Randomized Delayed-Start Trial of Levodopa in Parkinson's Disease. N Engl J Med. 2019; 380:315-324.
8. Dawson VL, Dawson TM: Promising disease-modifying therapies for Parkinson's disease. Sci Transl Med. 2019; 11.
9. Axelsen TM, Woldbye DPD: Gene Therapy for Parkinson's Disease, An Update. J Parkinsons Dis. 2018; 8:195-215; Bartus RT, Weinberg MS, Samulski RJ: Parkinson's disease gene therapy: success by design meets failure by efficacy. Mol Ther. 2014; 22:487-497.
10. Mok SW, Wong VK, Lo HH, de Seabra Rodrigues Dias IR, Leung EL, Law BY, et al: Natural products-based polypharmacological modulation of the peripheral immune system for the treatment of neuropsychiatric disorders. Pharmacol Ther. 2020; 208:107480.
11. Rai SN, Zahra W, Singh SS, Birla H, Keswani C, Dilnashin H, et al: Anti-inflammatory Activity of Ursolic Acid in MPTP-Induced Parkinsonian Mouse Model. Neurotox Res. 2019; 36:452-462; Perni M, Galvagnion C, Maltsev A, Meisl G, Muller MB, Challa PK, et al: A natural product inhibits the initiation of alpha-synuclein aggregation and suppresses its toxicity. Proc Natl Acad Sci U S A. 2017; 114:E1009-E1017.
12. Deng YN, Shi J, Liu J, Qu QM: Celastrol protects human neuroblastoma SH-SY5Y cells from rotenone-induced injury through induction of autophagy. Neurochem Int. 2013; 63:1-9.
13. Jiang M, Liu X, Zhang D, Wang Y, Hu X, Xu F, et al: Celastrol treatment protects against acute ischemic stroke-induced brain injury by promoting an IL-33/ST2 axis-mediated microglia/macrophage M2 polarization. J Neuroinflammation. 2018; 15:78.
14. Bian M, Du X, Cui J, Wang P, Wang W, Zhu W, et al: Celastrol protects mouse retinas from bright light-induced degeneration through inhibition of oxidative stress and inflammation. J Neuroinflammation. 2016; 13:50.
15. Cleren C, Calingasan NY, Chen J, Beal MF: Celastrol protects against MPTP- and 3-nitropropionic acid-induced neurotoxicity. J Neurochem. 2005; 94:995-1004.
16. Paris D, Ganey NJ, Laporte V, Patel NS, Beaulieu-Abdelahad D, Bachmeier C, et al: Reduction of beta-amyloid pathology by celastrol in a transgenic mouse model of Alzheimer's disease. J Neuroinflammation. 2010; 7:17; Veerappan K, Natarajan S, Ethiraj P, Vetrivel U, Samuel S: Inhibition of IKKbeta by celastrol and its analogues - an in silico and in vitro approach. Pharm Biol. 2017; 55:368-373.
17. Bakar MH, Sarmidi MR, Kai CK, Huri HZ, Yaakob H: Amelioration of mitochondrial dysfunction-induced insulin resistance in differentiated 3T3-L1 adipocytes via inhibition of NF-kappaB pathways. Int J Mol Sci. 2014; 15:22227-22257.

18. Sassa H, Takaishi Y, Terada H: The triterpene celastrol as a very potent inhibitor of lipid peroxidation in mitochondria. Biochem Biophys Res Commun. 1990; 172:890-897.
19. Angelopoulou E, Pyrgelis ES, Piperi C: Neuroprotective potential of chrysin in Parkinson's disease: Molecular mechanisms and clinical implications. Neurochem Int. 2020; 132:104612.
20. Linker RA, Lee DH, Ryan S, van Dam AM, Conrad R, Bista P, et al: Fumaric acid esters exert neuroprotective effects in neuroinflammation via activation of the Nrf2 antioxidant pathway. Brain. 2011; 134:678-692.
21. Olagnier D, Brandtoft AM, Gunderstofte C, Villadsen NL, Krapp C, Thielke AL, et al: Nrf2 negatively regulates STING indicating a link between antiviral sensing and metabolic reprogramming. Nat Commun. 2018; 9:3506; Buendia I, Michalska P, Navarro E, Gameiro I, Egea J, Leon R: Nrf2-ARE pathway: An emerging target against oxidative stress and neuroinflammation in neurodegenerative diseases. Pharmacol Ther. 2016; 157:84-104.
22. von Otter M, Bergstrom P, Quattrone A, De Marco EV, Annesi G, Soderkvist P, et al: Genetic associations of Nrf2-encoding NFE2L2 variants with Parkinson's disease - a multicenter study. BMC Med Genet. 2014; 15:131.
23. von Otter M, Landgren S, Nilsson S, Celojevic D, Bergstrom P, Hakansson A, et al: Association of Nrf2-encoding NFE2L2 haplotypes with Parkinson's disease. BMC Med Genet. 2010; 11:36.
24. Xiao H, Lv F, Xu W, Zhang L, Jing P, Cao X: Deprenyl prevents MPP(+)-induced oxidative damage in PC12 cells by the upregulation of Nrf2-mediated NQO1 expression through the activation of PI3K/Akt and Erk. Toxicology. 2011; 290:286-294.
25. Gan L, Vargas MR, Johnson DA, Johnson JA: Astrocyte-specific overexpression of Nrf2 delays motor pathology and synuclein aggregation throughout the CNS in the alpha-synuclein mutant (A53T) mouse model. J Neurosci. 2012; 32:17775-17787.
26. Luo D, Guo Y, Cheng Y, Zhao J, Wang Y, Rong J: Natural product celastrol suppressed macrophage M1 polarization against inflammation in diet-induced obese mice via regulating Nrf2/HO-1, MAP kinase and NF-kappaB pathways. Aging (Albany NY). 2017; 9:2069-2082.
27. Bae J, Lee D, Kim YK, Gil M, Lee JY, Lee KJ: Berberine protects 6-hydroxydopamine-induced human dopaminergic neuronal cell death through the induction of heme oxygenase-1. Mol Cells. 2013; 35:151-157.
28. Zhang B, Wang G, He J, Yang Q, Li D, Li J, et al: Icariin attenuates neuroinflammation and exerts dopamine neuroprotection via an Nrf2-dependent manner. J Neuroinflammation. 2019; 16:92.
29. Haque ME, Akther M, Jakaria M, Kim IS, Azam S, Choi DK: Targeting the microglial NLRP3 inflammasome and its role in Parkinson's disease. Mov Disord. 2019.
30. Wang S, Yuan YH, Chen NH, Wang HB: The mechanisms of NLRP3 inflammasome/pyroptosis activation and their role in Parkinson's disease. Int Immunopharmacol. 2019; 67:458-464.
31. Han X, Sun S, Sun Y, Song Q, Zhu J, Song N, et al: Small molecule-driven NLRP3 inflammation inhibition via interplay between ubiquitination and autophagy: implications for Parkinson disease. Autophagy. 2019; 15:1860-1881.

32. Lee E, Hwang I, Park S, Hong S, Hwang B, Cho Y, et al: MPTP-driven NLRP3 inflammasome activation in microglia plays a central role in dopaminergic neurodegeneration. Cell Death Differ. 2019; 26:213-228.
33. Yan Y, Jiang W, Liu L, Wang X, Ding C, Tian Z, et al: Dopamine controls systemic inflammation through inhibition of NLRP3 inflammasome. Cell. 2015; 160:62-73.
34. Xu LL, Wu YF, Yan F, Li CC, Dai Z, You QD, et al: 5-(3,4-Difluorophenyl)-3-(6-methylpyridin-3-yl)-1,2,4-oxadiazole (DDO-7263), a novel Nrf2 activator targeting brain tissue, protects against MPTP-induced subacute Parkinson's disease in mice by inhibiting the NLRP3 inflammasome and protects PC12 cells against oxidative stress. Free Radic Biol Med. 2019; 134:288-303.
35. Yang C, Mo Y, Xu E, Wen H, Wei R, Li S, et al: Astragaloside IV ameliorates motor deficits and dopaminergic neuron degeneration via inhibiting neuroinflammation and oxidative stress in a Parkinson's disease mouse model. Int Immunopharmacol. 2019; 75:105651.
36. Dai W, Wang X, Teng H, Li C, Wang B, Wang J: Celastrol inhibits microglial pyroptosis and attenuates inflammatory reaction in acute spinal cord injury rats. Int Immunopharmacol. 2019; 66:215-223.
37. Xin W, Wang Q, Zhang D, Wang C: A new mechanism of inhibition of IL-1beta secretion by celastrol through the NLRP3 inflammasome pathway. Eur J Pharmacol. 2017; 814:240-247.
38. Sofroniew MV: Astrocyte barriers to neurotoxic inflammation. Nat Rev Neurosci. 2015; 16:249-263.
39. Hickman S, Izzy S, Sen P, Morsett L, El Khoury J: Microglia in neurodegeneration. Nat Neurosci. 2018; 21:1359-1369.
40. Charvin D, Medori R, Hauser RA, Rascol O: Therapeutic strategies for Parkinson disease: beyond dopaminergic drugs. Nat Rev Drug Discov. 2018; 17:844.
41. Park JS, Leem YH, Park JE, Kim DY, Kim HS: Neuroprotective Effect of beta-Lapachone in MPTP-Induced Parkinson's Disease Mouse Model: Involvement of Astroglial p-AMPK/Nrf2/HO-1 Signaling Pathways. Biomol Ther (Seoul). 2019; 27:178-184.
42. Zhu J, Hu Z, Han X, Wang D, Jiang Q, Ding J, et al: Dopamine D2 receptor restricts astrocytic NLRP3 inflammasome activation via enhancing the interaction of beta-arrestin2 and NLRP3. Cell Death Differ. 2018; 25:2037-2049.
43. Cheng Q, Shen Y, Cheng Z, Shao Q, Wang C, Sun H, et al: Achyranthes bidentata polypeptide k suppresses neuroinflammation in BV2 microglia through Nrf2-dependent mechanism. Ann Transl Med. 2019; 7:575.
44. von Herrmann KM, Salas LA, Martinez EM, Young AL, Howard JM, Feldman MS, et al: NLRP3 expression in mesencephalic neurons and characterization of a rare NLRP3 polymorphism associated with decreased risk of Parkinson's disease. NPJ Parkinsons Dis. 2018; 4:24.
45. Konieczny J, Jantas D, Lenda T, Domin H, Czarnecka A, Kuter K, et al: Lack of neuroprotective effect of celastrol under conditions of proteasome inhibition by lactacystin in in vitro and in vivo studies: implications for Parkinson's disease. Neurotox Res. 2014; 26:255-273.
46. Jackson-Lewis V, Przedborski S: Protocol for the MPTP mouse model of Parkinson's disease. Nat Protoc. 2007; 2:141-151.

47. Zheng R, Yang L, Sikorski MA, Enns LC, Czyzyk TA, Ladiges WC, et al: Deficiency of the RIIβ subunit of PKA affects locomotor activity and energy homeostasis in distinct neuronal populations. Proc Natl Acad Sci U S A. 2013; 110:E1631-1640.
48. Yun SP, Kam TI, Panicker N, Kim S, Oh Y, Park JS, et al: Block of A1 astrocyte conversion by microglia is neuroprotective in models of Parkinson's disease. Nat Med. 2018; 24:931-938.
49. Tsai PT, Hull C, Chu Y, Greene-Colozzi E, Sadowski AR, Leech JM, et al: Autistic-like behaviour and cerebellar dysfunction in Purkinje cell Tsc1 mutant mice. Nature. 2012; 488:647-651; Sampson TR, Debelius JW, Thron T, Janssen S, Shastri GG, Ilhan ZE, et al: Gut Microbiota Regulate Motor Deficits and Neuroinflammation in a Model of Parkinson's Disease. Cell. 2016; 167:1469-1480 e1412.
50. Wang S, Peng Z, Wang S, Yang L, Chen Y, Kong X, et al: KRAB-type zinc-finger proteins PITA and PISA specifically regulate p53-dependent glycolysis and mitochondrial respiration. Cell Res. 2018; 28:572-592; Huang Y, Xu Z, Xiong S, Sun F, Qin G, Hu G, et al: Repopulated microglia are solely derived from the proliferation of residual microglia after acute depletion. Nat Neurosci. 2018; 21:530-540.
51. Nam JH, Park ES, Won SY, Lee YA, Kim KI, Jeong JY, et al: TRPV1 on astrocytes rescues nigral dopamine neurons in Parkinson's disease via CNTF. Brain. 2015; 138:3610-3622.
52. Giordano N, Iemolo A, Mancini M, Cacace F, De Risi M, Latagliata EC, et al: Motor learning and metaplasticity in striatal neurons: relevance for Parkinson's disease. Brain. 2018; 141:505-520.
53. Jantas D, Roman A, Kusmierczyk J, Lorenc-Koci E, Konieczny J, Lenda T, et al: The extent of neurodegeneration and neuroprotection in two chemical in vitro models related to Parkinson's disease is critically dependent on cell culture conditions. Neurotox Res. 2013; 24:41-54.
54. Ahuja M, Ammal Kaidery N, Yang L, Calingasan N, Smirnova N, Gaisin A, et al: Distinct Nrf2 Signaling Mechanisms of Fumaric Acid Esters and Their Role in Neuroprotection against 1-Methyl-4-Phenyl-1,2,3,6-Tetrahydropyridine-Induced Experimental Parkinson's-Like Disease. J Neurosci. 2016; 36:6332-6351.
55. Chen PC, Vargas MR, Pani AK, Smeyne RJ, Johnson DA, Kan YW, et al: Nrf2-mediated neuroprotection in the MPTP mouse model of Parkinson's disease: Critical role for the astrocyte. Proc Natl Acad Sci U S A. 2009; 106:2933-2938.
56. Lastres-Becker I, Garcia-Yague AJ, Scannevin RH, Casarejos MJ, Kugler S, Rabano A, et al: Repurposing the NRF2 Activator Dimethyl Fumarate as Therapy Against Synucleinopathy in Parkinson's Disease. Antioxid Redox Signal. 2016; 25:61-77; Jo MG, Ikram M, Jo MH, Yoo L, Chung KC, Nah SY, et al: Gintonin Mitigates MPTP-Induced Loss of Nigrostriatal Dopaminergic Neurons and Accumulation of alpha-Synuclein via the Nrf2/HO-1 Pathway. Mol Neurobiol. 2019; 56:39-55.
57. Chen Y, Zhang QS, Shao QH, Wang S, Yuan YH, Chen NH, et al: NLRP3 inflammasome pathway is involved in olfactory bulb pathological alteration induced by MPTP. Acta Pharmacol Sin. 2019; 40:991-998.
58. Qiao C, Zhang LX, Sun XY, Ding JH, Lu M, Hu G: Caspase-1 Deficiency Alleviates Dopaminergic Neuronal Death via Inhibiting Caspase-7/AIF Pathway in MPTP/p Mouse Model of Parkinson's Disease. Mol Neurobiol. 2017; 54:4292-4302.

59. Zhou Y, Lu M, Du RH, Qiao C, Jiang CY, Zhang KZ, et al: MicroRNA-7 targets Nod-like receptor protein 3 inflammasome to modulate neuroinflammation in the pathogenesis of Parkinson's disease. Mol Neurodegener. 2016; 11:28.
60. Cheng J, Liao Y, Dong Y, Hu H, Yang N, Kong X, et al: Microglial autophagy defect causes parkinson disease-like symptoms by accelerating inflammasome activation in mice. Autophagy. 2020:1-13.
61. Zhu X, Liu J, Huang S, Zhu W, Wang Y, Chen O, et al: Neuroprotective effects of isoliquiritigenin against cognitive impairment via suppression of synaptic dysfunction, neuronal injury, and neuroinflammation in rats with kainic acid-induced seizures. Int Immunopharmacol. 2019; 72:358-366.
62. Pires AO, Teixeira FG, Mendes-Pinheiro B, Serra SC, Sousa N, Salgado AJ: Old and new challenges in Parkinson's disease therapeutics. Prog Neurobiol. 2017; 156:69-89; Elkouzi A, Vedam-Mai V, Eisinger RS, Okun MS: Emerging therapies in Parkinson disease - repurposed drugs and new approaches. Nat Rev Neurol. 2019; 15:204-223.
63. Koprich JB, Kalia LV, Brotchie JM: Animal models of alpha-synucleinopathy for Parkinson disease drug development. Nat Rev Neurosci. 2017; 18:515-529.
64. Athauda D, Maclagan K, Skene SS, Bajwa-Joseph M, Letchford D, Chowdhury K, et al: Exenatide once weekly versus placebo in Parkinson's disease: a randomised, double-blind, placebo-controlled trial. Lancet. 2017; 390:1664-1675.
65. Cheng L, Quek CY, Hung LW, Sharples RA, Sherratt NA, Barnham KJ, et al: Gene dysregulation is restored in the Parkinson's disease MPTP neurotoxic mice model upon treatment of the therapeutic drug Cu(II)(atsm). Sci Rep. 2016; 6:22398; Fresard L, Smail C, Ferraro NM, Teran NA, Li X, Smith KS, et al: Identification of rare-disease genes using blood transcriptome sequencing and large control cohorts. Nat Med. 2019; 25:911-919.
66. Fao L, Mota SI, Rego AC: Shaping the Nrf2-ARE-related pathways in Alzheimer's and Parkinson's diseases. Ageing Res Rev. 2019; 54:100942; Zhang L, Hao J, Zheng Y, Su R, Liao Y, Gong X, et al: Fucoidan Protects Dopaminergic Neurons by Enhancing the Mitochondrial Function in a Rotenone-induced Rat Model of Parkinson's Disease. Aging Dis. 2018; 9:590-604; Liddell JR: Are Astrocytes the Predominant Cell Type for Activation of Nrf2 in Aging and Neurodegeneration? Antioxidants (Basel). 2017; 6.
67. Guo H, Callaway JB, Ting JP: Inflammasomes: mechanism of action, role in disease, and therapeutics. Nat Med. 2015; 21:677-687.
68. Heneka MT, Kummer MP, Stutz A, Delekate A, Schwartz S, Vieira-Saecker A, et al: NLRP3 is activated in Alzheimer's disease and contributes to pathology in APP/PS1 mice. Nature. 2013; 493:674-678; Mao Z, Liu C, Ji S, Yang Q, Ye H, Han H, et al: The NLRP3 Inflammasome is Involved in the Pathogenesis of Parkinson's Disease in Rats. Neurochem Res. 2017; 42:1104-1115.
69. Lau A, So RWL, Lau HHC, Sang JC, Ruiz-Riquelme A, Fleck SC, et al: alpha-Synuclein strains target distinct brain regions and cell types. Nat Neurosci. 2020; 23:21-31.

70. Jiang P, Dickson DW: Parkinson's disease: experimental models and reality. Acta Neuropathol. 2018; 135:13-32.

Figures

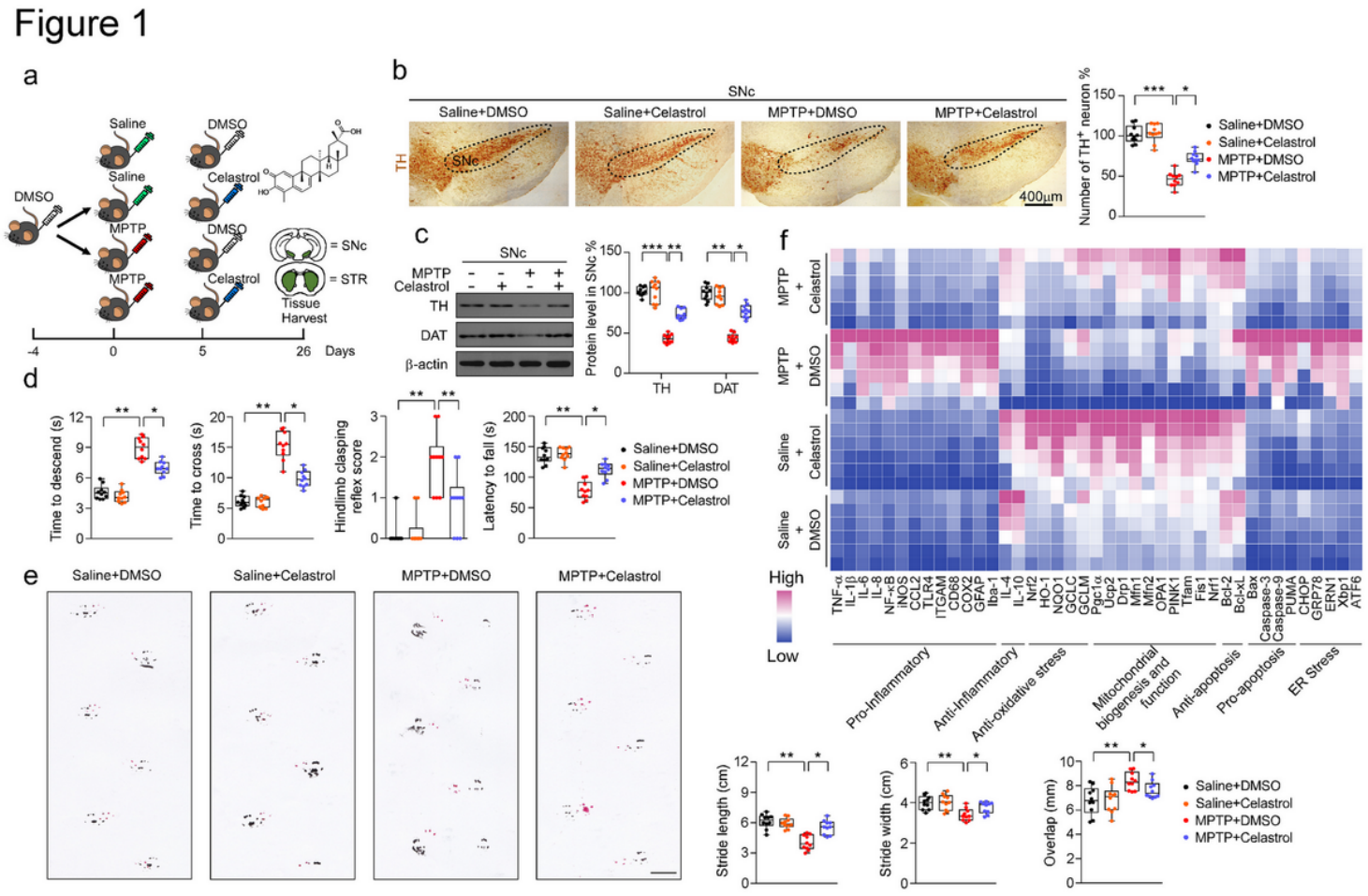

Figure 1

Neuroprotective effects of celastrol in MPTP-induced PD mouse model. a Diagram of the experimental design. MPTP (20 mg/kg□or vehicle (saline) was injected (i.p.) for 5 consecutive days starting on day -4 after acclimation (3 days), then mice intraperitoneally (i.p.) treated celastrol (10 μg/kg) or vehicle (DMSO) per day for 7, 14, 21 days, and finally tissues were harvested for molecular analyses at day 26 after the last behavior test. b Representative photomicrographs and unbiased stereological counts of TH staining in SNc, Scale bars 400 μm. Data are mean ± s.e.m.; n = 10 from three independent experiments. c Protein levels of TH, DAT and β-actin in SNc. Data are mean ± s.e.m.; n = 10 from three independent experiments. d Time to traverse beam apparatus, time to descend pole, Hind-limb clasping reflex score, fall latency

from an accelerating rotarod and gait analysis (e). Data are mean ± s.e.m.; n = 10 biologically independent animals. f Relative mRNA expression of the indicated genes in SNc. Data are mean ± s.e.m.; n = 8 biologically independent animals. The one-way ANOVAs were used for statistical analysis followed by Bonferroni's post hoc test. *P < 0.05, **P < 0.01, and ***P < 0.001. ns, not significant.

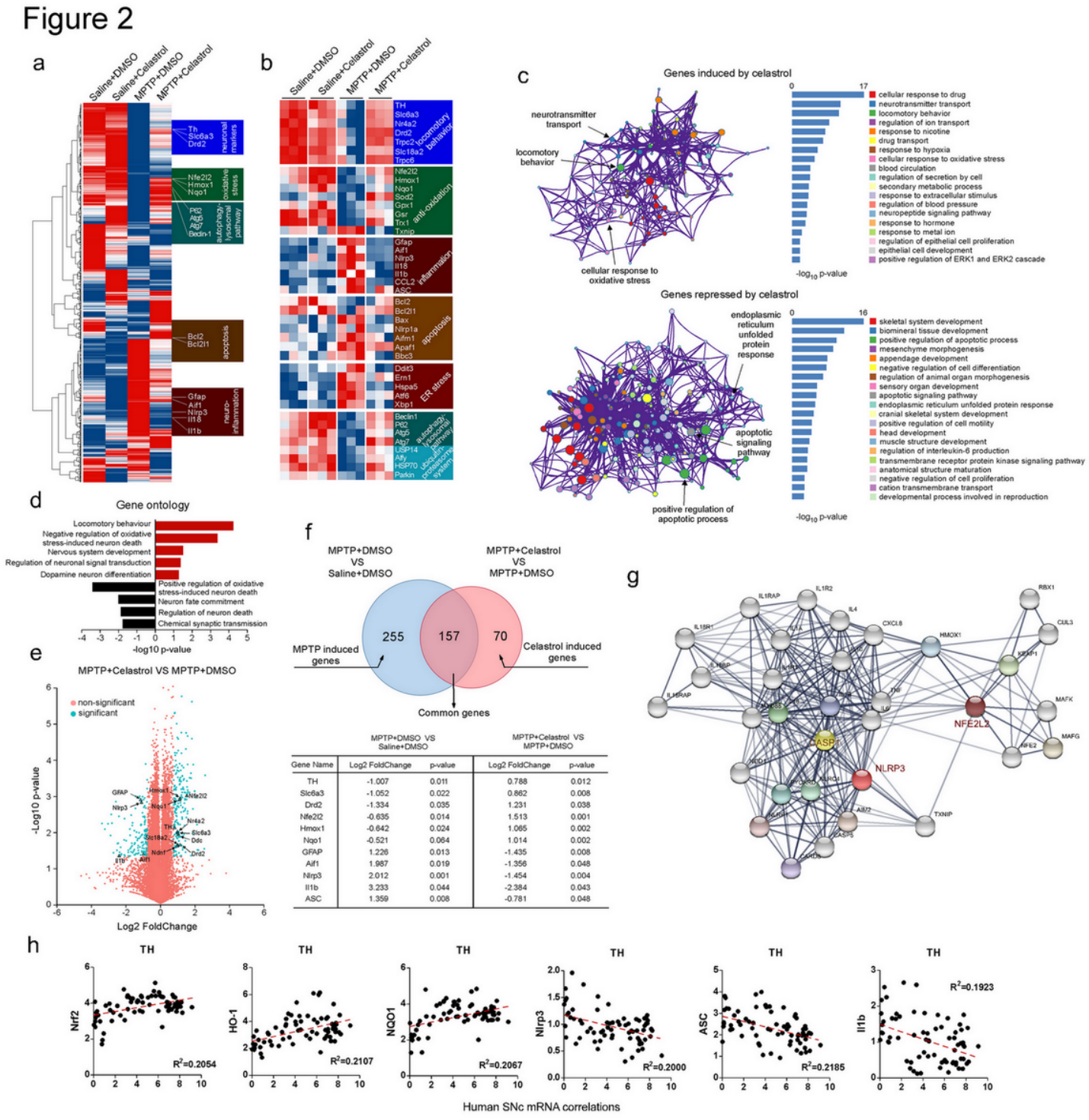

Figure 2

Gene profiles analysis of SNc in MPTP-induced PD mice treated with celastrol. a Hierarchical clustered heatmap of gene expression profiles for celastrol or vehicle treatment in SNc under the condition of

MPTP injection. b Heatmap of DEGs of MPTP-received mice treated with celastrol or vehicle. c KEGG analysis highlights the DEGs of celastrol treatment compared with vehicle in MPTP-recieved mice, upregulated genes are colored in red, downregulated genes are colored in blue. (P < 0.05 with unpaired two-tailed Student's t-tests). d Gene Ontology enrichment was based on DEGs that have a P value smaller than 0.05. Enrichment analysis for Gene Ontology terms among the genes of a gene–trait correlation module was performed using Metascape. e Volcano plot displays DEGs of celastrol treatment compared with vehicle in MPTP-received mice. Significantly altered genes are colored in red, insignificantly altered genes are colored in blue. f Venn diagram of overlapping significantly changed genes (± 1.2 fold, P < 0.05). The top ten overlapping genes are presented in diagram. g Protein–protein interaction network identified among Nrf2, NLRP3 and Caspase1 using STRING database.

Figure 3

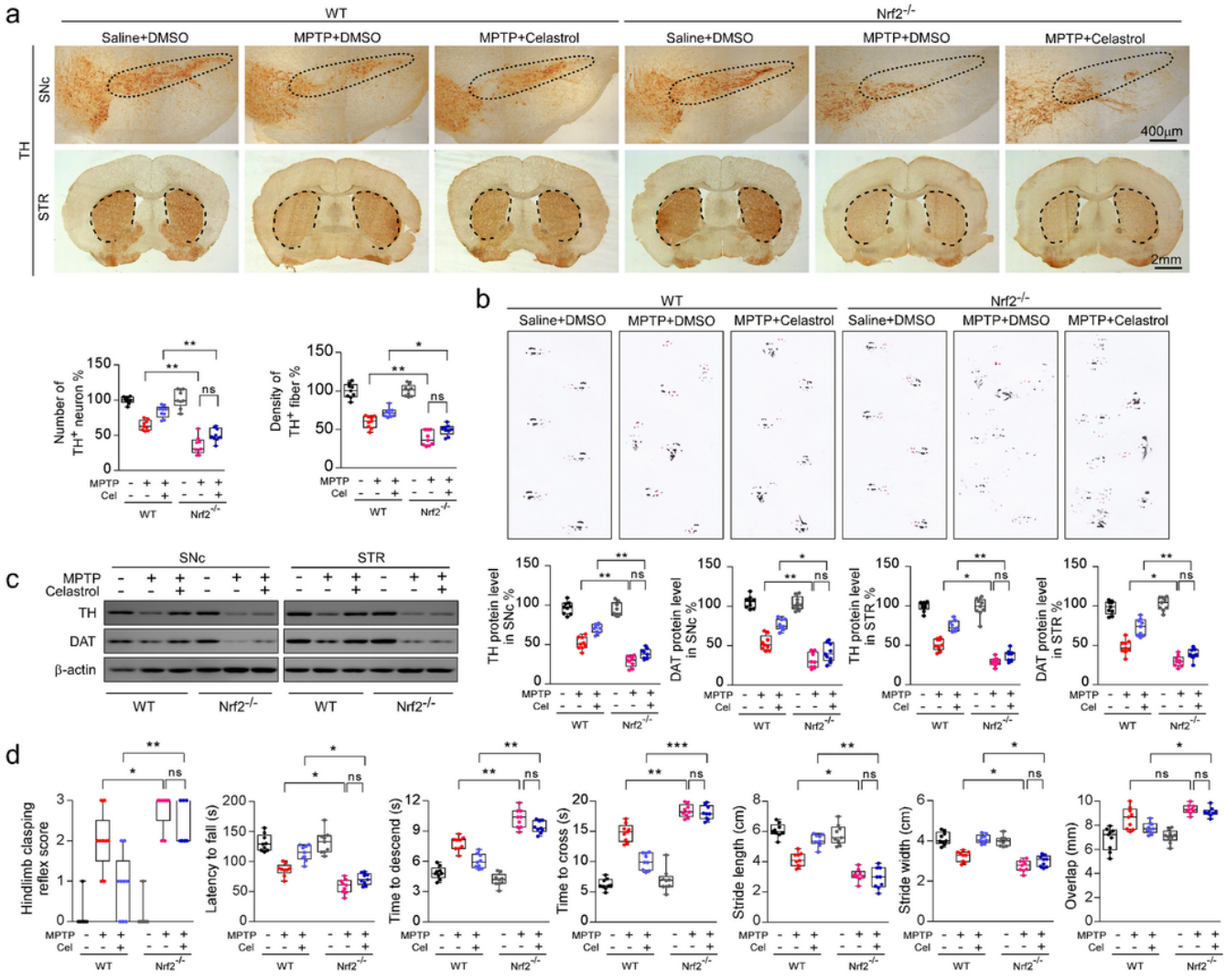

Figure 3

Neuroprotective effects of celastrol in PD are Nrf2 dependent. a Representative TH staining of SNc and STR, unbiased stereological counts of TH+ neurons in SNc and the quantity of TH+ striatal fiber density

in STR of WT and Nrf2-KO mice in WT and Nrf2-KO mice, scale bar, 400 μm for SNc, 2 mm for STR. b Representative diagram of gait test of WT and Nrf2-KO mice treated with celastrol or vehicle. c Representative immunoblots and quantification of TH, DAT in SNc or STR levels of WT and Nrf2-KO mice. Data are mean ± s.e.m.; n = 9 from three independent experiments. d Time to traverse beam apparatus, time to descend pole, hind-limb clasping reflex score, fall latency from an accelerating rotarod. Data are mean ± s.e.m.; n = 9 from three independent experiments. Two-way ANOVA followed by Tukey's post hoc test. *P < 0.05, **P < 0.01, and ***P < 0.001. ns, not significant.

Figure 4

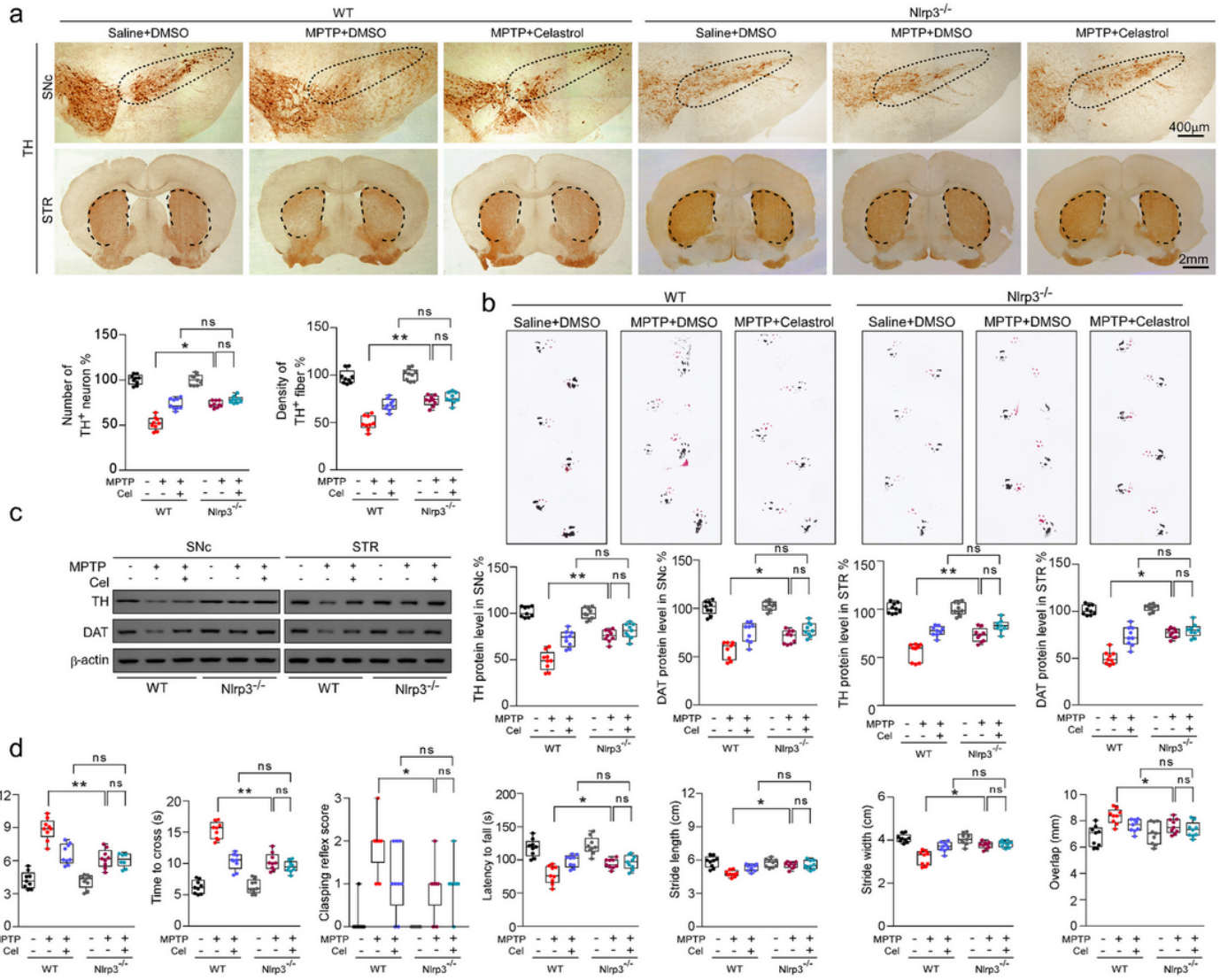

Figure 4

Neuroprotective actions of celastrol A in PD are mediated by Nrf2-NLRP3 axis. a Representative TH staining of SNc and STR, unbiased stereological counts of TH+ neurons in SNc and the quantity of TH+ striatal fiber density in STR of WT and NLRP3-KO mice in WT and NLRP3-KO mice, scale bar, 400 μm for SNc, 2 mm for STR . b Representative diagram of gait test of WT and NLRP3-KO mice treated with

celastrol or vehicle. c Representative immunoblots and quantification of TH, DAT levels in SNc or STR of NLRP3-KO mice. Data are mean ± s.e.m.; n = 9 from three independent experiments. d Time to traverse beam apparatus, time to descend pole, hind-limb clasping reflex score, fall latency from an accelerating rotarod. Data are mean ± s.e.m.; n = 9 from three independent experiments. Two-way ANOVA followed by Tukey's post hoc test. *P < 0.05, **P < 0.01, and ***P < 0.001. ns, not significant.

Figure 5

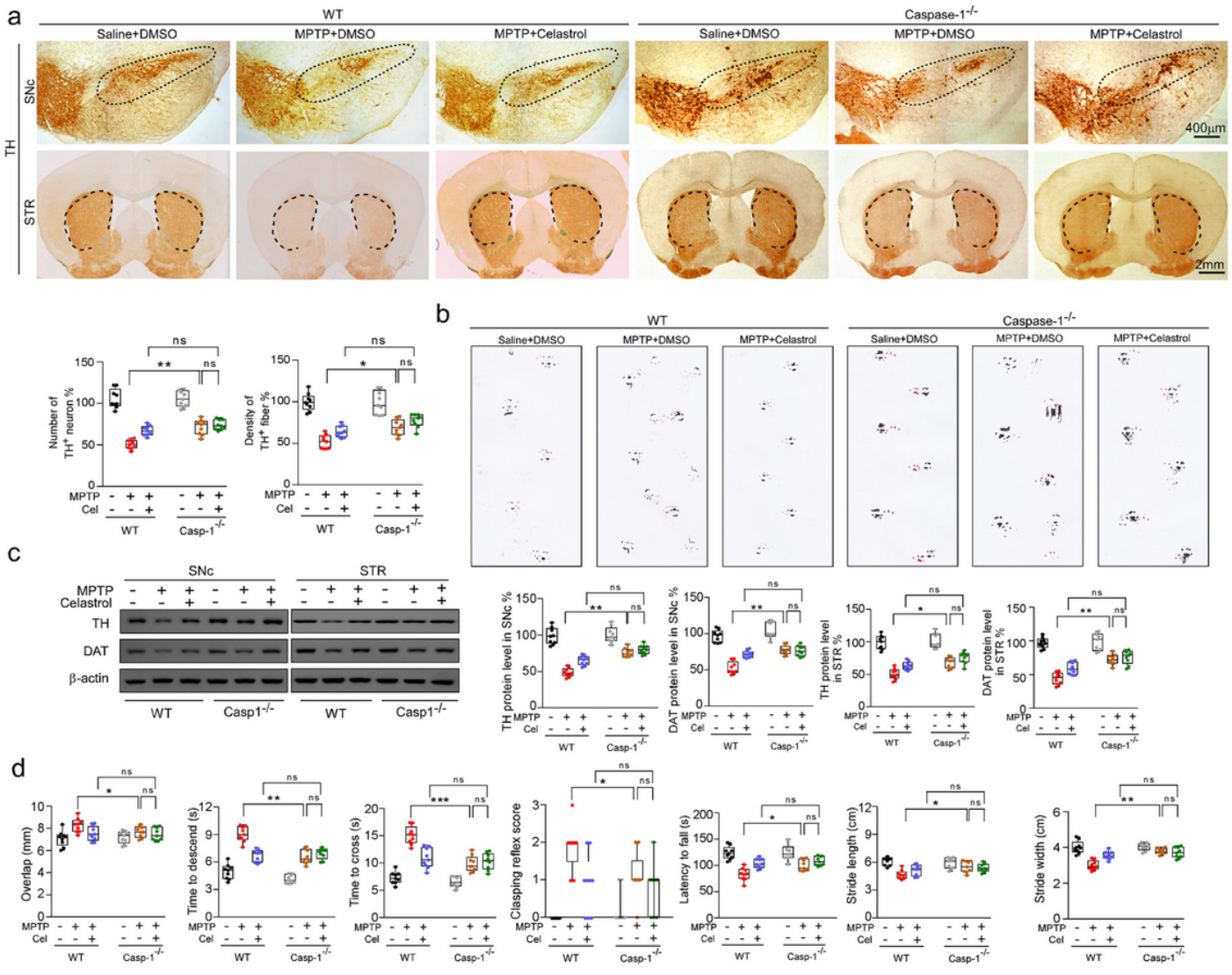

Figure 5

Celastrol suppresses Caspase1 to protect dopaminergic neurons from MPTP neurotoxicity. a Representative TH staining of SNc and STR in WT and Caspase1-KO mice, unbiased stereological counts of TH+ neurons in SNc and the quantity of TH+ striatal fiber density in STR of WT and Caspase1-KO mice, scale bar, 400 μm for SNc, 2 mm for STR. b Representative diagram of gait test of WT and Caspase1-KO mice treated with celastrol or vehicle. c Representative immunoblots and quantification of TH, DAT levels in SNc or STR of WT and Caspase1-KO mice. Data are mean ± s.e.m.; n = 9 from three independent experiments. d Time to traverse beam apparatus, time to descend pole, hind-limb clasping

reflex score, fall latency from an accelerating rotarod. Data are mean ± s.e.m.; n = 9 from three independent experiments. Two-way ANOVA followed by Tukey's post hoc test. *P < 0.05, **P < 0.01, and ***P < 0.001. ns, not significant.

Figure 6

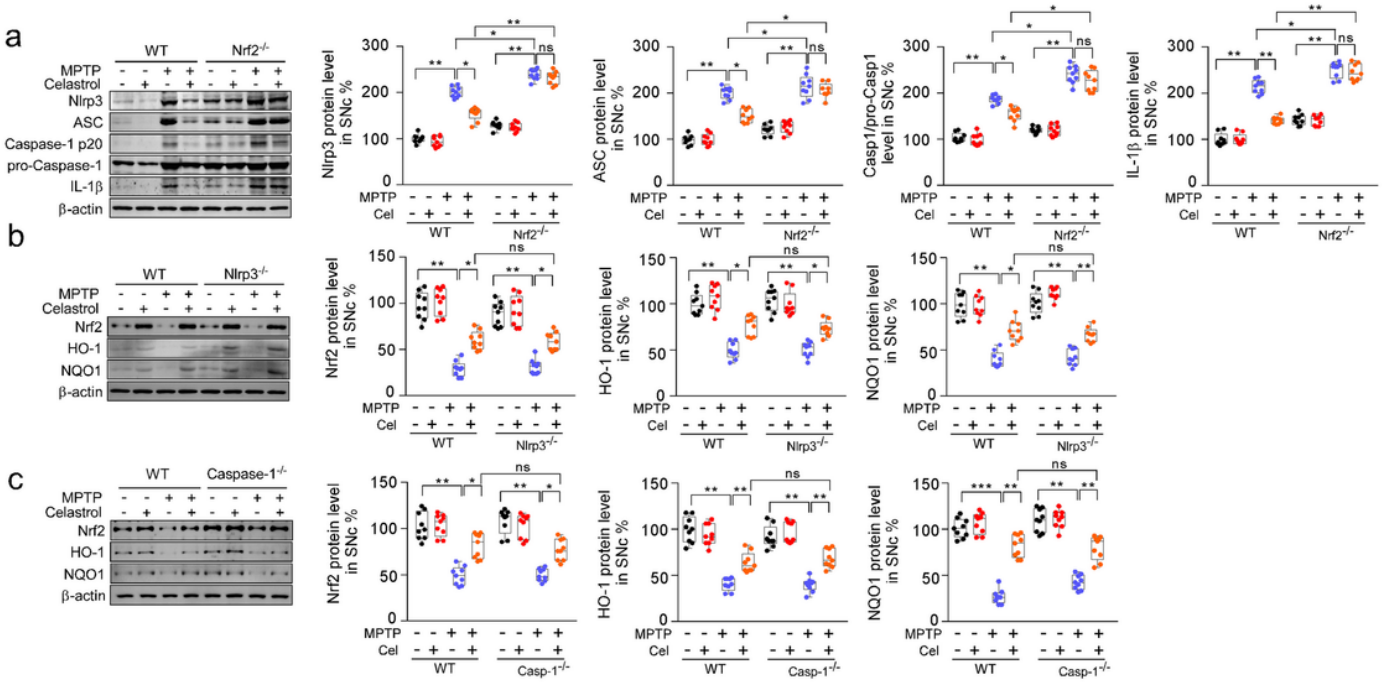

Figure 6

The effects of celastrol are mediated by Nrf2-NLRP3-Caspase1 axis. a Representative immunoblots and quantification of protein levels in SNc of Nrf2-KO mice. Data are mean ± s.e.m.; n = 9 from three dependent experiments. i Representative immunoblots and quantification of protein levels in SNc of NLRP3-KO mice. Data are mean ± s.e.m.; n = 9 from three dependent experiments. b Representative immunoblots and quantification of protein levels in SNc of Caspase1-KO mice. Data are mean ± s.e.m.; n = 9 from three dependent experiments. c Correlation of TH with Nrf2, HO1, NQO1, NLRP3, ASC and Iba1 in the human SNc by gene network. *P < 0.05, **P < 0.01, and ***P < 0.001 by two-way ANOVAs followed by Tukey's multiple comparisons test.

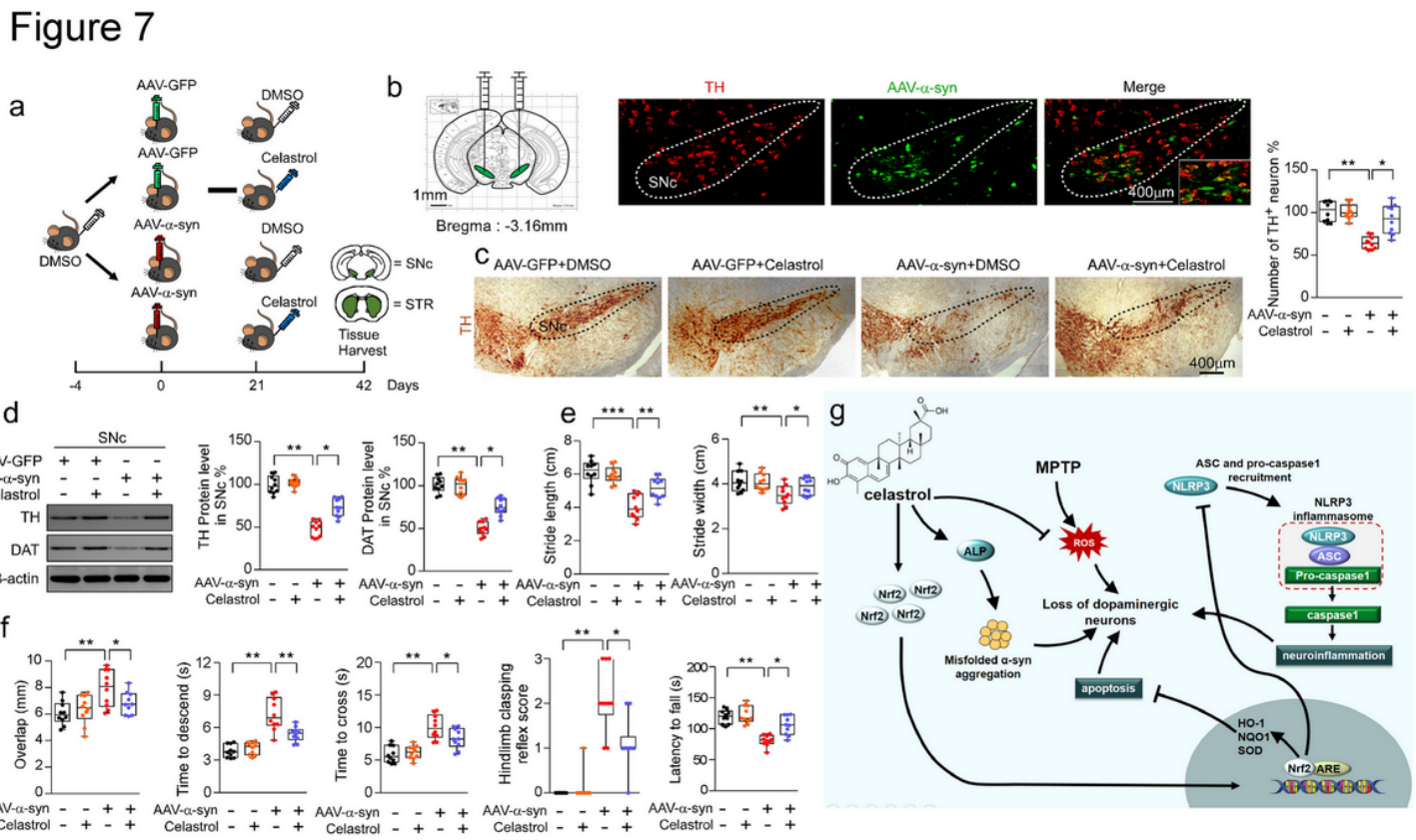

Figure 7

Celastrol protects against the loss of dopaminergic neurons in human α-syn overexpressing mice. a Diagram of the experimental design. b Representational diagram of AAV injection site in mice and the co-labelling of TH with human-α-syn showed that human-α-syn mainly expressed within the SNc dopaminergic neurons. c Representative TH staining and quantification of SNc dopaminergic neurons in human α-syn over-expressing mice treated with celastrol. Scale bar 400 μm. Data are mean ± s.e.m.; n = 10 from three independent experiments. d Protein levels of TH, DAT and β-actin in SNc of mice treated with celastrol or vehicle under the condition of MPTP. Data are mean ± s.e.m.; n = 10 from three independent experiments. e, f Time to traverse beam apparatus, time to descend pole, hind-limb clasping reflex score, fall latency from an accelerating rotarod and gait analysis. Data are mean ± s.e.m.; n = 10 from three independent experiments. *P < 0.05, **P < 0.01 and ***P < 0.001 by one-way ANOVA with Bonferroni's post hoc test. g Schematic summary of the mechanism underlying the neuroprotective actions of celastrol in PD.

Supplementary Files

This is a list of supplementary files associated with this preprint. Click to download.

- SupplementaryFigure1.tif
- SupplementaryFigure2.tif

- SupplementaryFigure3.tif
- SupplementaryFigure4.tif
- SupplementaryFigure5.tif
- SupplementaryFigure6.tif
- SupplementaryFigure7.tif
- SupplementaryFigure8.tif
- SupplementaryFigure9.tif
- SupplementaryFigure10.tif
- SupplementaryFigure11.tif
- SupplementaryFigure12.tif
- SupplementaryFigure13.tif
- SupplementaryFigure14.tif
- SupplementaryFigure15.tif
- SupplementaryFigure16.tif
- SupplementaryFigure17.tif
- SupplementaryFigure18.tif
- SupplementaryFigure19.tif